Research Square

Preprints are preliminary reports that have not undergone peer review.
They should not be considered conclusive, used to inform clinical practice,
or referenced by the media as validated information.

WITHDRAWN: Cytotoxicity and wound healing efficacy of biosynthesis ZnO Nanoparticles Using Aspergillus niger against Multidrug Resistant Pseudomonas aeruginosa

Elham E. Moustafa
elham.mostafa@women.asu.edu.eg
Ain Shams University
Maha A. Hewedy
Ain Shams University
Salah Abdelbary
Al-Azhar University
Howida R. Mohammed
Ain Shams University
Zeinab M.H. Kheiralla
Ain Shams University

Research Article

Keywords: Burns, Multidrug resistant Pseudomonas aeruginosa, Biosynthesis, ZnO Nanoparticles, and Wound healing

Posted Date: October 18th, 2023

DOI: https://doi.org/10.21203/rs.3.rs-3445222/v1

License: This work is licensed under a Creative Commons Attribution 4.0 International License. Read Full License

Additional Declarations: No competing interests reported.

EDITORIAL NOTE:

The full text of this preprint has been withdrawn by the authors while they make corrections to the work. Therefore, the authors do not wish this work to be cited as a reference. Questions should be directed to the corresponding author.

Abstract

Background

Critically ill patients, particularly burn patients, are at substantial risk from *Pseudomonas aeruginosa* infection, which is a common source of healthcare-acquired infections. The rise of multidrug resistant pathogens is increasing, making control difficult. Infectious infections continue to be a public health concern worldwide, owing to growing resistance to antimicrobial agents. The current study was designed to assess the effectiveness of biologically produced zinc oxide nanoparticles (ZnO-NPs) *in* both *vitro* and *vivo* against *MDR P. aeruginosa*.

Results

Four soil samples were gathered from various sites. Fifteen fungus isolates were identified and tested for their ability to produce green ZnO NPs. The antibacterial activity of the biosynthesized ZnO NPs was evaluated against *P. aeruginosa*. Using morphological and molecular methods, a powerful fungal isolate in producing ZnO NPs was identified. The isolate of the fungus was recognized as *A. niger*. ZnO-NPs were produced biologically and UV-vis spectroscopy, Fourier-transform infrared (FT-IR), Transmission Electron Microscopy (TEM), X-ray diffraction (XRD), and Zeta potential and particle size analysis were then used to characterize the samples. The biosynthesized ZnO NPs had no impact on normal melanocyte mammalian cell line (Hfb4) with IC_{50} 365.64μM, had an antitumor effect on breast cancer cell lines (Mcf7) with IC_{50} 61.92μM and displayed antiviral effects against the herpes simplex virus type 1 (Hvs1) (91.4%) at 250 μg/ml. Using female albino rats infected with *P. aeruginosa*, the antibacterial efficacy and wound healing effectiveness of synthesized ZnO NPs were assessed and their activity was compared with different agents including saline solution alone, fusidic acid (20 ml/g), and chemically synthesized ZnO NP. In comparison to other agents employed, the findings demonstrated that biosynthesized ZnO NPs have a significant impact on the process of wound healing. An estimation of the oxidative stress and immune response in rats given biosynthesized ZnO NP treatments revealed that oxidative stress and inflammation were reduced because of the presence of infection. Three weeks later, histopathological examination was performed to assess the wound healing development.

Conclusions

The outcomes showed after 14 days, ZnO NPs are highly effective against MDR *P. aeruginosa* and accelerate the healing of wounds.

Background

Despite the advances in understanding pathogenesis of microorganisms and the use of contemporary therapies, the morbidity and mortality associated with microbial infections remain significant. The increased rate of infectious diseases and drug resistance bacteria reached an alarming level [1]. Regardless

of the severity of the burns, infection is still the leading cause of death for patients with burns [2]. Bacteria, fungi, and/or viruses can all cause burn wound infections. Burn patients are more vulnerable of developing hospital-associated infections because burn injuries alter the immune system's physiological function and weaken the skin's barrier against infection [3]. One of the most common pathogenic agents found in burn sites and causing serious infections is *Pseudomonas aeruginosa* [4]. It was extremely difficult for burn patients because of the immune suppression that occurs in burn patients as well as the preference of *P. aeruginosa* for moist and warm wound settings [5, 6]. Increased antibiotic resistance is shown in *P. aeruginosa. Pseudomonas aeruginosa* that are resistant to three or more kinds of anti-Pseudomonal antimicrobials is known as multidrug-resistant (MDR) phenotype [7].

Nanoparticles work effectively against germs that are resistant to antibiotics, are less toxic, and are heat resistant. Numerous techniques, including physical, chemical, and biological ones, are used to create nanoparticles [8]. When it comes to massive scale development, precisely defined and nanostructures that are stable as well as the attraction of nanoscale particles, physical and chemical approaches offer various benefits. The limits of the physical technique include the requirement for expensive equipment, extraordinary temperatures and pressures, and enormous machine setup areas. One of the downsides of the chemical approach is the use of toxic chemicals that are harmful to individuals as well as the environment [9]. Nanoparticle production utilizing plants or microorganisms is referred to as "biosynthesis of nanoparticles." Antibacterial, anticancer, anti-aging, antioxidant, and anti-biofilm inhibition and anti-inflammatory therapies are all properties of nanoparticles produced using such "green synthesis" processes [10].

Fungi are highly prospects for the creation of metal nanoparticles since they are eukaryotic creatures. The fungus produces well-defined dimensions and nanoparticles with excellent mono dispersity. In investigations on the biological synthesis of metallic nanoparticles, fungi are gaining center stage due to their tolerance and capacity for metal bioaccumulation [11]. Fungi are exceptionally effective extracellular enzyme secretors, making it simple to get large-scale synthesis of enzymes [12]. Additional advantages of using a green technique mediated by fungi to produce metallic nanoparticles include economic viability and ease of biomass management. The genetic manipulation of eukaryotic organisms to increase the expression of particular enzymes is comparatively much more challenging in prokaryotes than it is in eukaryotes, which is a key disadvantage of employing these bio-entities in the production of nanoparticles.

The biological method of the ZnO NPs synthesis is gaining importance due to its simplicity, eco-friendliness and extensive antimicrobial activity [13]. In mice, these particles effectively reduce skin infection, bacterial load, and inflammation while also improving infected skin [14]. As a result, creative methodologies and new antimicrobial compounds produced from natural and inorganic components are necessary for the development of the next generation of drugs or agents to control microbial illnesses.

In this study, ZnO NPs were synthesized utilizing biological synthesis mediated by fungi, characterized, and their antibacterial efficacy against vital and harmful diseases was evaluated such as multi-drug resistant *P. aeruginosa* isolated from burn infection. Also, *in vivo* evaluate the activity of the biosynthesized ZnO nanoparticles for wound recovery.

Results and discussions

Isolation of fungal isolates

Total of fifteen filamentous fungal isolates were isolated from different sites. Morphological and microscopic characteristics were observed and were found to be belonging to 3 divisions:Zygomycotina (*Rhizopus sp.* and *Mucor sp.*), Ascomycotina (*Aspergillus sp.* and *Pencillium sp.*) and Deutromycotina (*Fusarium sp.*).

Screening of the isolated fungi for zinc oxide nanoparticle production

All isolated fungi were tested for their ability to produce zinc oxide nanoparticles. The results of the biosynthesis of zinc oxide nanoparticles from freshly prepared cell free supernatant of different fungal isolates. The change of color to white precipitate indicates the formation of ZnO NPs. The optical absorption spectra of green synthesized ZnO NPs were measured using UV-vis spectrophotometer with a wavelength range of 200–800 nm as a primary characterization to confirm the biosynthesis of ZnO NPs, from 15 fungal isolates; 14 isolates were in the range of 200- 800nm. The results showed that a broad absorption band located around 270 nm indicated the formation of ZnO NPs (Fig. 1). An appropriate approach for confirming and characterizing the production of ZnO NPs constructed on surface plasmon resonance (SPR) was used to characterize the optical characteristics of ZnO NPs using a UV-Vis spectrophotometer [15].

Figure 1. UV- spectroscopy of the biosynthesized ZnO NPs by the isolated fungi.

Identification of a powerful fungal isolate for biosynthesis of ZnO nanoparticles

Macroscopic and Microscopic Examination of Isolated Fungi

The morphology of the most potent fungus F14 for biosynthesis of ZnO NPs was observed macroscopically, the colony features such as color, shape, size and hyphae, following by the slide culture technique. Figures (2) indicated that, diameter of colonies on C′zapek agar was 5-7cm when incubated for 7 days at 28^{o}C. Growing quickly, seeming black with the observed color and a pale-yellow reverse. Conidia sub-globose are 3.5 µm in diameter. Conidial heads were black and had a radiate form on the 28.0 µm diameter vesicle.

Figure 2. The morphological characteristics of a powerful fungus for biosynthesis of ZnO NPs where A; forward side and B; reverse side

b. Molecular identification of most potent fungal isolates producing ZnO NPs

The isolate F14, displayed a high degree of similarity (99%) to *Aspergillus niger*, according to phylogenetic analysis as shown in Table (1) and Figure (3&4).

Figure 3. Gel electrophoresis of the most potent fungal isolate F14

Table 1.

Table 1
Similarity percentage scores of 18SrDNA sequencing of fungal isolate compared to those obtained from database.

Similar organisms	Identity % according to nucleotides
Aspergillus niger strain NR58	100
Aspergillus niger strain 110	100
Aspergillus niger strain ND58	100
Aspergillus niger isolate WA-TKA	99.7
Aspergillus niger strain 7M1	99.7

Figure 4. Phylogenetic tree created using the 18s rDNA sequencing of the fungus isolate code F14, related to Aspergillus niger with accession number OR603165.

Optimization of Aspergillus niger growth for the biosynthesis of ZnO NPs

Zinc Oxide NPs were entirely synthesized outer the fungal cell using *A. niger* biomass. Zn^{+2} ions in zinc acetate are converted into ZnO NPs via reduction, which results in the development of white colour at the end of the reaction. These outcomes coincided with those mentioned by **Kalpana et al.** [16] who synthesized ZnO NPs after 48 hours, the colour of the *A. niger* culture filtrate was altered from pale yellow to clear by combining it with an aqueous solution of zinc nitrate. Because of the proteins reducing zinc nitrate ions, white precipitate of ZnO NPs is produced. **Shamim et al.** [17] stated that *A. niger* has the capability to synthesize ZnO NPs both extracellularly and intracellularly, however extracellular synthesis has greater potential. Extracellular synthesis is mediated by enzymes like nitrate reductase, which is released in the medium and changes metal ions into metal NPs. When an enzyme called NADH reductase transfers electrons from NADH to Zn^{+2}, which are afterwards reduced to become ZnO NPs. Microorganisms have the capacity to produce NPs, and this process is a very effective substitute for chemical and physical processes. Utilizing microorganisms to boost yield production on an industrial scale raises significant challenges that need for further research. The form and size of NPs have a significant impact on their physicochemical characteristics. The direct correlation between NPs' size and shape and performance has been demonstrated in numerous research. Therefore, the need to improve both culture environment and many physical characteristics that affect how effectively NPs are produced in terms of size distribution, morphologies, and yield including pH, temperature, precursor concentration, inoculum size, and incubation period. Optimization of different growth factors of *A. niger* mycelium for the production of ZnO NPs were determined to select the optimum condition such as pH, temperature, inoculum size, incubation period, and

precursor concentration. The optimum conditions for the biosynthesis of ZnO NPs that had high efficacy against MDR *P. aeruginosa* strain were pH 6, temperature 20^{o}C, incubation period at 5 days, inoculum size (5 discs) and precursor concentration at 5mM as shown in Figures (5 a, b. c, d and e).

Figure 5. Effect of A. niger growth conditions on the antimicrobial activity of the biosynthesized of ZnO NPs against MDR P.aeruginosa strain.

Automated optimization by Taguchi system

The Taguchi design is a statistical method built on orthogonal arrays that enables the evaluation of combined impact of multiple factors as well as the identification of the ideal conditions while only requiring a small number of experiments [18, 19]. The optimum values of different growth factor of *A. niger* were inserted in Taguchi system with ± 2. The system gave 25 runs with different conditions for biosynthesized ZnO NPs nanoparticles, UV-spectroscopy was used to pre-characterize these runs and also evaluated ZnO NPs for antibacterial properties against MDR *P. aeruginosa* to inhibit its growth (Table 2). The optimum values that exhibited the highest antimicrobial activity was temp. (30^{o}C), pH (6), inoculum size (2 discs), precursor concentration (5mM) and incubation time (3 days).

Table 2
UV- spectroscopy and antimicrobial activity of ZnO NPs.

Runs	UV Absorbance (200–800)	Inhibition zone diameter (mm) of *P. aeruginosa*
1	2.23 ± 0.861	5.93 ± 0.367
2	1.41 ± 0.684	9.76 ± 0.476
3	1.05 ± 0.591	23.3 ± 0.483
4	0.36 ± 0.348	27.5 ± 0.919
5	0.24 ± 0.281	27.6 ± 0.688
6	0.93 ± 0.557	24.16 ± 0.645
7	2.75 ± 0.957	23.63 ± 0.876
8	0.55 ± 0.427	21.96 ± 0.779
9	0.45 ± 0.387	6.93 ± 0.526
10	0.35 ± 0.339	11.06 ± 0.519
11	0.79 ± 0.514	25.63 ± 0.549
12	2.41 ± 0.895	8.26 ± 0.539
13	1.67 ± 0.745	20.2 ± 0.900
14	0.26 ± 0.294	22.5 ± 0.620
15	0.50 ± 0.406	24.2 ± 0.240
16	0.23 ± 0.274	20.73 ± 0.951
17	1.00 ± 0.577	9 ± 0.480
18	0.91 ± 0.551	23.4 ± 0.754
19	1.32 ± 0.664	22.2 ± 0.822
20	0.43 ± 0.379	10.67 ± 0.342
21	0.66 ± 0.468	5.8 ± 0.240
22	0.67 ± 0.473	26.1 ± 0.929
23	1.05 ± 0.593	8.46 ± 0.519
24	0.21 ± 0.267	6.1 ± 0.346
25	1.14 ± 0.615	21.5 ± 0.779

Table 2.

The MIC of biosynthesized ZnO NPs against MDR Pseudomonas aeruginosa.

MIC value of the biosynthesized ZnO NPs against *Pseudomonas aeruginosa* was achieved to be 2mM of zinc acetate. **Mekky et al.** [20] indicated that MICs values of biosynthesized ZnO NPs by *A. niger* against *P. aeruginosa* was 50 µg/ml.. **Shah et al.** [21] reported that ZnO-NPs produced by *A. niger* may have an inhibitory effect because of their high surface-to-volume ratio, or their impact on intracellular protein leakage and cell membrane permeability, which inhibits growth [22–24]. Additionally, NPs prevent bacterial development by inhibiting cell proteins through a reaction with thiol (-SH) groups [25]. Additionally, probably as a result of its interaction with DNA's phosphorus group, which prevents DNA replication and, as a result, prevents protein synthesis [26, 27]. NPs may affect biochemical procedures by generating reactive oxygen species (ROS), which can harm biological elements like lipids, DNA, and proteins and finally obstruct development [28].

Characterization of the biosynthesized ZnO NPs.

The construction of biosynthesized ZnO NPs were confirmed by UV-Vis spectroscopy measurement that indicated a strong absorption band around 270 nm in the ultraviolet region which indicated the formation of ZnO NPs (Fig. 6a). In contrast to, **Hefny et al**. [29] who discovered that all ZnO nanoparticles produced by the examined fungi (*Aspergillus niger, Aspergillus tubulin, Aspergillus fumigatus, Penicillium citrinum*, and *Fusarium oxysporum*) had a significant absorption peak between 285 and 296 nm.. Also, **Es-haghi et al.** [30] demonstrated that the UV–Vis absorption spectra of green synthesized ZnO-NPs showed an absorption peak at 320 nm.

As represented Fig. 6b, X-ray diffraction patterns showed the three strongest and narrow reflections at positions of around *2θ* 32.1°, 34.5°, and 36.5° suggesting that (100), (002), (101), and (102) crystallographic reflections are revealed the hexagonal structure (hcp) of zinc oxide atoms has a lattice-spacing distance (dhkl) of 2.8, 2.6, and 2.5 A^{o}, respectively. The XRD results of the biosynthesized ZnO NPs patterns were enclose agreement with **Rasha et al.** [31] who recorded that XRD pattern of the *Aspergillus niger* ZnO-NPs showed that the ZnO-NP peaks were located at 2 of 31.77°, 34.44°, and 36.26° which corresponded to the (100), (002), (101) lattice planes

Fourier transform infrared spectroscopy **(**FT-IR) provides information about the makeup and development of functional groupings of ZnO nanoparticles that have been synthesized. Also, ascertain the potential interactions between biologically active molecules and ZnO NPs, this might be the reason of the composition and stabilization of ZnO NPs. The many unique functional groups related to the synthesized nanoparticles were discovered using the FT-IR analysis of the biosynthesized ZnO NPs (Fig. 6c). The peaks represent the functional groups that are characteristic of the biosynthesized zinc oxide nanoparticles. The sample was discovered to have absorption peaks in the scale 3889, 3833, 3778, 3631, 3262, 2889, 2832, 2776, 2665, 2498, 2060, 1882, 1825, 1635, 1104, 1048, 992, 937,677, 653, 597, 563, 545, 498, 480, 468, 449 and 428 cm^{-1}. The peaks at 3631 and 3262 cm^{-1} were supposed to be caused by the OH stretching H-bonded alcohols and phenols. The peaks at 2889, and 2832 indicated the presence of aldehyde C-H. The alkyl C = C stretch was responsible for the peak at 1635 cm^{-1}. The C-N stretching vibrations led to the formation of the band at 1048 cm^{-1}. The peaks in the 400–900 cm^{-1} range (992, 937, 677, 653, 597, 563, 545, 498, 480, 468, 449, and 428 cm^{-1}), which show the origin and purity of the ZnO structure, are caused

by the stretching mode of ZnO. ZnO was shown to exist when stretched at 480 cm^{-1}, whereas metal oxides are present in spectra with wavenumbers below 500 cm^{-1}. The ZnO stretching mode is responsible for the 400–900 cm^{-1} range of the peaks, demonstrating the formation and purity of the ZnO structure [32]. Our finding was in accordance with **Chen et al.** [33] **and Ashwini et al.** [34] who noticed that ZnO is present, as seen by the stretching at 485 cm^{-1}.

The TEM image appeared that ZnO NPs have diameters ranging from 16 to 27 nm and exhibited hexagonal quartzite with a crystalline form(Fig. 6d) according to TEM results of **Hefny et al.** [29] indicated that *Aspergillus niger*-ZnO-NPs, *Aspergillus tubulin*-ZnO-NPs, *Aspergillus fumigatus*-ZnO-NPs, *Penicillium citrinum*-ZnO-NPs and *Fusarium oxysporum*- ZnO-NPs displayed a crystalline structure with a hexagonal wurtzite form (30–100 nm size). Finally, the stability of ZnO suspensions was proven using measurements of the zeta potential and particle size (Fig. 6e), the ZnO-NPs had a mean Z-average diameter 94.4 nm was larger than what was determined using TEM images. The zetasizer study's heterogeneous dispersion of ZnO nanoparticles increased particle size in colloidal solution [35]. As stated by **Gao et al.** [36], ZnO NPs produced by *A. niger* reached in size from 80 to 130 nm and were shaped practically like rods and clusters. The biosynthesized ZnO NPs had a potential value of -16.5 mV, because to high electrostatic repulsive forces, they were exceedingly stable and resisted aggregation. Our result is in accordance with **Mekky et al.** [20] who found ZnO NPs made from *Aspergillus niger* extracellular extracts have zeta potential (η) of roughly − 14.4 ± 4.75 mV. The compounds in the extract have a strong affinity for attaching to metallic ions, provides the particles their scattering stability and avoids accumulation, is what causes the particles' negative surface charge [37, 38]. **Manosalva et al.** [39] considered that stable nanoparticles are produced by zeta potential ranging from + 30 mV to -30 mV.

Figure 6. Characterization of the biosynthesized ZnO NPs utilizing A. niger; a) UV-Vis spectra, b) XRD, c) FTIR, d) TEM, and e) Zeta size and Zeta potential.

Cytotoxicity assay of ZnO NPs using (MTT) Assay protocol

Viability tests are critical for determining the cellular response to toxicants. The MTT test was performed to assess overall cell viability after NPs treatment. Due to physical and chemical properties, zinc oxide is considered an effective agent in cancer therapy. A novel approach of biosynthesis ZnO NPs using a natural source, such as fungal biomass to reduce metal ions which are ecofriendly and nontoxic compared with physical and chemical methods. Cellular defense mechanisms are engaged when nanoparticles contact with cells to reduce the damaging effect [40]. However, it is not widely known whether ZnO NPs from the filamentous fungus *A. niger* have any anticancer properties [36]. Figure 7A and C revealed, the exposure of normal skin cell line Hfb4 to biosynthesized and chemically synthesized ZnO NPs disclosed that cytotoxicity of ZnO NPs decreased with decreasing the concentration, with half maximal inhibitory concentrations (IC_{50}) 365.64 and 94.6 for the biosynthesized and chemical ZnO NPs, respectively. The biosynthesized was less cytotoxic than that of chemical prepared ZnO NPs. While biosynthesized ZnO NPs were effective on the proliferation of the breast cancer (MCF7) cells with IC_{50} 61.92µM compared with 248.72µM for chemically synthesized ZnO NPs, (Fig. 7B and D) which in agreement with **Sayed et al.** [41] who discovered that dose-dependent effects were observed MCF7 and HepG2 cancer cells treated with

varied dosages of ZnO NPs had a decrease in viability and a steady increase in toxicity. Because of this, "green" or biosynthesized nanoparticles (NPs) exhibit greater stability and activity than NPs made using more traditional methods [42]. The results suggest that the *A. niger* mediated ZnO NPs can effectively suppress the growth of studied cancer cell. Similar findings have been reported by **Padalia and Chanda** [43] **and Gomathi et al.** [44], whereby the capability of green ZnO-NPs to destroy cancer cells has been demonstrated. Furthermore, ZnO-NPs have been observed to disintegrate within the lysosome and donate Zn^{2+} ions [45]. These ions have a role in scavenging ROS [46].

Figure 7. The impact of chemically synthesized ZnO NPs (A and C) and biosynthesized ZnO NPs by A.niger (B and D) on Hfb4 and Mcf-7cell lines at different concentrations.

Antiviral activity of biosynthesized ZnO NPs

During the pathogenesis process, Zn-induced Zn^{2+} ions may play a role affects viral growth control and may finally trigger viral death in host cells. Given that they have a strong human cell biocompatibility, ZnO nanoparticles (NPs) have attracted the most attention among all nanoparticle types. ZnO NPs have direct antiviral effect against a variety of viruses because they can stop viral entrance, reproduction, and dissemination to organs. They can also eventually cause reactive oxygen species to be produced, which causes oxidative damage and viral death [47]. A life-long infection is represented by the herpes-simplex virus type-1 (HSV1). Acyclovir is the main treatment, however as resistant strains are on the rise, new treatment methods are becoming necessary. Therapeutics based on ZnO NPs are attracting a lot of interest. Herpes virus infection of cultured corneas is prevented by ZnO-NPs [48], lowered the viral titer as well as 92% of the virus's rate [49]. Changes on the surface of ZnO NPs may impair a virus's ability to infect cells by neutralizing the viral rather than obstructing its cellular targets. According to **Ghaffari et al.** [50], Zn^{2+} ions may prevent viral reproduction and increase the amount of intracellular Zn^{2+} that can effectively stop the replication of many RNA viruses. It is thought that nanoparticles could represent a new class of antibacterial and antiviral agents. The results in Table 3 also showed that ZnO NPs produced through biosynthesis could inhibit HSV1 with an antiviral efficacy of 91.4% at 250 µg/ml, compared to ZnO NPs produced through chemical synthesis, which had an antiviral impact of 67% at 62.5 µg/ml. These outcomes concurred with those that were previously published by **El-Megharbel et al.** [51] who demonstrated that direct synthesised ZnO NPs exhibit strong antiviral activity at low doses (IC_{50} = 526 ng/ml) but also some cytotoxic effect to the cell host by (CC_{50} = 292.2ng/ ml).

Table 3
Antiviral activity of ZnO NPs on Herpes-simplex virus type-1 (Hsv1).

Test	Concentration (µM/ml)	Mean OD ± SDE	Viability	Toxicity	Viral activity (%)	Antiviral effect (%)
Control (Vero)	0	0.655 ± 0.010642	100	ND	ND	ND
HSV1	0	0.259 ± 0.004444	39.54198473	60.45801527	100	0
A	62.5	0.524333 ± 0.019763	80.05089059	19.94910941	32.99663	67.003367
B	250	0.621 ± 0.011	94.80916031	5.190839695	8.585859	91.41414141
A: chemically synthesized ZnO NPs B: biosynthesized ZnO NPs						

Table 3.

Application ZnO NPs in vitro/ in vivo

In vitro, Efficacy of different antimicrobial agents against MDR P. aeruginosa

Table 4 exhibited the antibacterial activity of different antimicrobial agents indicated that *Pseudomonas aeruginosa* was affected only by the biosynthesized ZnO NPs with a diameter of inhibition zone 12.2 ± 0.339 mm while, chemical synthesis ZnO NPs, zinc acetate in dist. H_2O, dist. H_2O alone and antibiotic fusidic acid (20mg/100ml) had no effect. **Kelly et al.** [52] **and Siddiqi et al.** [53] demonstrated that ZnO NPs have high permeability via binding to lipids and proteins to the cytoplasmic membrane and cell wall. Lipids, carbohydrates, proteins, and DNA become damaged as a result of the oxidative stress. Because zinc oxide is inherently amphoteric, it may interact with both acids and alkalis to create Zn^{2+} ions, which bind right away to biomolecules like proteins and carbohydrates and all of a bacterium's vital functions. This resulting in concerns about the toxicity of nanoparticles that release noxious ions.

Table 4
Efficacy of different antimicrobial agents against MDR *Pseudomonas aeruginosa.*

	Diameter of inhibition zone(mm)				
	Biological ZNO NPs (MIC)	Chemical ZNO NPs (MIC)	Antibiotic fusidic acid (20mg)	Zinc acetate in dist. H2O	Dist. H2O
Pseudomonas aeruginosa	12.2 ± 0.339	0	0	0	0

Table 4.

ZnO-NPs Improve MDR P. aeruginosa-Infected Wound Healing in Rats

The antibacterial and wound-healing abilities of biosynthesized ZnO NPs were examined and compared with different agents such as saline solution, fusidic acid with a concentration 20 ml/g, and chemical synthesis ZnO NPs using one group of female albino rats, GI infected with *P. aeruginosa* (Fig. 8). Macroscopic observation after 7 days showed the presence of high inflammation and more pus cells in sub-groups GIa (wounded, infected and treated with saline). After 14 days, in comparison to other agents used, the findings showed that the biosynthesized ZnO NPs significantly effect on the wound healing process.

Figure (8): Efficacy of different antimicrobial agents against P. aeruginosa.

Biochemical and Immunological analysis

Zinc is a fundamental component in superoxide dismutase (SOD). **Prasad** [54] **and Abd El-Hack et** [55, 56] revealed that SOD participates in the cellular removal of ROS and free radicals. Malondialdehyde (MDA), a marker of lipid peroxidation and the oxidative harm brought on by ROS, is crucial. Our results support the notion that nano-ZnO at the right concentrations stimulates SOD activity, and that increased SOD will inhibit ROS formation and lower MDA levels. The effect of biosynthesized synthesis ZnO NPs on female albino rats infected with MDR *P. aeruginosa* and compared with other antimicrobial agents was illustrated in Table (5). The subgroups treated with biosynthesis ZnO NPs, Lipid peroxide (Malondialdehyde) (MDA) showed oxidative stress is decreasing due to the presence of infection by MDR *Pseudomonas aeruginosa*; the highest mean of MDA level was in GIa (wounded, infected, and treated with saline) at 5.23 ± 0.257 n.mol/mg/protein, respectively and the lowest mean of MDA was in GIc (wounded, infected and treated with biosynthesized ZnO NPs) at 1.32 ± 0.260, respectively, there is a reduction in oxidative stress and increasing in SOD as a response of immune system to fight the infection in wound area compared with other treatments in rat models. On other hand, **Tang et al.** [57] reported that ZnO nanoparticles decreased SOD activity and liver's overall antioxidant capacity. The results showed an increasing in superoxide dismutase (SOD) as a response of immune system to fight the infection in the wound area compared to other treatments in rat models; the highest mean of SOD level was in GIc (wounded, infected, and treated with biosynthesized ZnO NPs) at 3.81 ± 0.27 U/mg/protein and the lowest mean of SOD was in GIa (wounded, infected and treated with saline) at 1.11 ± 0.44.

Moreover, pro-inflammatory cytokines (TNF-α and IL-1β) levels were significantly reduced in GIc (wounded, infected and treated with biosynthesized ZnO NPs), that represent a sign that the process of healing a wound is progressing. The comparison between the subgroups showed that the GIc (wounded, infected and treated using biosynthesized ZnO NPs) revealed a notable drop in pro-inflammatory cytokines, IL-1β, TNF-α and this was evidence of the progress of the wound healing process. These results are in agreement with **Li et al.** [58] who discovered that the use of ZnO NPs significantly reduces oxidative stress in animals with inflammation and suppresses pro-inflammatory cytokines including IL-1β and TNF- α. while **Abass et al.** [59] found comparatively to both control groups (a negative control group did not receive any therapy, while a positive control group got 1 ml of deionized water), the ZnO NPs administrated group showed pro-inflammatory cytokines IL-1 β, TNF- α and INF- have significantly increased ($P < 0.001$ for each). The

ability of ZnO-NPs to produce reactive nitrogen species, as well as the overexpression of cyclooxygenase (Cox-2), induced nitric oxide synthase (iNOS), pro-inflammatory cytokines (IL-6, IFN-, TNF-, IL-17, and regulatory cytokine IL-10), and mitogen-activated protein kinase (MAPKS), which were found to be inhibited after blocking internalization of ZnO NPs through caveolae receptor pathway may be the mechanism for their anti-inflammatory effects [60, 61].

Table 5.

Table 5
Physiological and Immunological analysis of rat model infected with MDR *P.aeruginosa.*

Parameter	Healthy group	Control (wounded, uninfected and untreated)	GIa (Saline)	GIb (Antibiotic (fusidic acid 20mg))	GIc (Biosynthesised ZnO NPs)	GId (Chemically ZnO NPs)
MDA (n.mol/mg/protein)	0.82 ± 0.109	3.40 ± 0.305	5.23 ± 0.257	3.03 ± 0.316	1.32 ± 0.260	2.28 ± 0.216
SOD (u/mg/protein)	4.23 ± 0.441	1.47 ± 0.216	1.11 ± 0.444	1.84 ± 0.271	3.81 ± 0.271	2.67 ± 0.255
TNFα (pg/mg/protein)	86.54 ± 1.267	218.39 ± 1.078	289.08 ± 1.987	191.79 ± 1.087	121.20 ± 1.254	147.04 ± 1.313
IL-1 β (pg/mg/protein)	56.21 ± 1.372	316.01 ± 1.87	408.69 ± 0.863	280.99 ± 1.152	173.33 ± 1.546	201.52 ± 1.311

General Wound Healing Histopathology

Using one set of female albino rats afflicted with *P. aeruginosa*, the wound healing effectiveness of the biosynthesized ZnO NPs was done *in vivo*. This group divided into 4 sub- groups and treated with saline solution, fusidic acid with concentration 20 mg, biological and chemical synthesized ZnO NPs. Using H and E staining to determine the soft tissue recovery rate and wound healing of rat skin following four treatments was also assessed. On days 7, 14, and 21 following wounding, rats' new wounds were changed and their degree of closure was measured to determine the effectiveness of wound healing.

The GIa (wounded, infected and treated with saline) after 7 days revealed significant tissue inflammation along with the presence of pus cells. Also, the other 3 subgroups (GIb, GIc and GId) showed tissue inflammation with presence of pus cells. After 14 days, the outcomes demonstrated that, in comparison to other treatments used, synthesised ZnO NPs significantly affect how quickly wounds heal (Fig. 9). These findings corroborated those of **Rasha et al.** [31] who demonstrated that G-4, which received ZnO-NP ointment treatment, showed good outcomes in relation to the region where the wound was still healing, whilst G-3 (impenem-treated infected wound skin) shown intermediate healing. These outcomes might be brought about by the tested bacteria's resistance to imipenem. The wound healing rates for G-1 (untreated wounded skin) and G-2 (infected untreated wounded skin) were the slowest, which may be because they depended on an immune response to heal. Results of granulation/healing tissue sections stained with HE on days 7, 14, and 21 from the four test subgroups showed that wound areas of GIa had modest

immunological response recovery, while GIb (wounded, infected and treated with antibiotic), GId (wounded, infected and administered chemical ZnO NPs), the wound demonstrated intermediate curing due to the presence of the tested bacteria. However, the results shown that the best wound closure outcome in GIc (wounded, infected and administered biological ZnO NPs. The most notable finding from the photographs of the histology findings on days 7, 14, and 21 following injury was GIc. After 7 days, compared to the other therapies, it demonstrated enhanced wound healing and lower bacterial inflammation. These outcomes support the conclusions of numerous earlier investigations into the closure of infected wounds and using ZnO NPs [62] who studied that investigation of the ZnO NPs for wound healing revealed they were successful, indicating their potential to function as an efficient antiseptic tissue cement and further the outcome of **Gao et al.** [63] who indicated that ZnO NPs remain acceptable for treating tissue damage caused by a bacterial infection and are safe as determined by the Food and Drug Administration (FDA) [64].

Figure 9: **Rat skin photomicrographs showing a granulomatous response and a haemorrhage (red and blue arrows, respectively) (A) (wounded, infected, and treated with saline), (B) (wounded, infected, and treated with fusidic acid (20mg/100ml), (C) (wounded, infected, and treated with the biosynthesized ZnO NPs) and (D) (wounded, infected, and treated with the chemical ZnO NPs).**

Materials

Multi-drug resistant *Pseudomonas aeruginosa* strain used in this study was obtained from the Central Microbiology Laboratory of El-Demerdash Hospital, Cairo, Egypt and identified biochemically using VITEK 2® Compact automated system (Bio Mérieux, Marcy l'Etoile, France), and molecularly by 16S RNA in previous research [65].

Methods

Fungi for the biosynthesis of ZnO NPs: Isolation and Screening

In the Women Faculty for Arts, Science, and Education, Ain Shams University's, four soil samples were collected from Botany Department. Isolation and enumeration of fungi were performed using potato dextrose agar (g/l); 20 Dextrose, 4 potato extract and 15 agar according to **Waksman** [66] **and Rajaet al.** [67]. All fungal isolates were screened to detect the efficient isolates for ZnO NPs production. Malt glucose yeast peptone (MGYP) broth (g/l); 3 Malt extract, 3 yeast extract, 5 peptone, 10 glucose to cultivate each fungal isolate and yield biomass. Further incubation in an orbital shaker at 30°C for 5 days at 150 rpm, Whatman filter paper No.1 was used for collecting each fungal biomass and deionized water was used to wash it completely. The fungus biomass was put into 100ml of deionized water and further incubated at 150 rpm for 72 h. After filtering the sample, the cell-free filtrate was utilized. to create ZnO nanoparticles by combining 10 ml of 1mM Zinc acetate to 10 ml of each fungus filtrate (1:1) and adjusting the pH to 6.5 and incubating at 30ºC for 72 h at 150 rpm in a dark condition. Finally, the white color produced in the flasks

indicates the reduction process [68, 29]. The biosynthesized ZnO NPs were first characterized using UV-visible spectroscopy with a wavelength range of 200–800 nm.

Antibacterial activity

Using the agar well diffusion technique [69], the antibacterial activity of all biosynthesized ZnO NPs was assessed. The plates were inoculated with 200µl containing 2 x10^6 CFU/ml of fresh cultures of MDR *P. aeruginosa* and left to dry at room temperature, The wells were filled with different volumes (50, 100, 150, 200, 250 µl) of the biosynthesized ZnO NPs. Sterilized distilled water of zinc acetate (1mM/100 ml) was tested as control [29]. The plates were kept for 2h at 4°C to permit homogenous diffusion of the antimicrobial agent and then incubated for 24h at 37°C. The formation of a distinct inhibitory zone surrounding biosynthesized ZnO NPs [70].

Identification of the selected fungal isolate

Based on based on cultural and morphological characteristics, the chosen isolate was identified according to standard manuals [71, 72]. An image analysis system (Olympus BX 40) and Soft-Imaging GmbH software (analysis Pro. ver.3.0) at the Regional Center for Mycology and Biotechnology (RCMB), Al- Azhar University, Cairo, Egypt, was used to macroscopic and microscopic examinations to study the culture characteristics.

Afterward, DNA sample was isolated from the fungal isolate through Easy Pure Genomic DNA Extraction Kit city and country. The DNA sample was subjected to a PCR reaction achieved for 18s rDNA gene amplification of fungal isolate by using two universal fungal primer: FW5-ATGGGCAAGGCACCAAATAA-3 and RW 5 TGGAAATGGATCCAAGAATG-3.

The amplified product was visualized as a single compact band of the expected size using UV- gel documentation system (manufacturer, city and country). In order to purify and sequence the gel from the amplified PCR products were submitted to Solgent Co Ltd (South Korea). In Geneious software (Biomatters add version), the resulting sequences were trimmed and combined. As a result, the trimmed sequences were found using the basic local alignment search tool (BLAST) in the Gene Bank database of the National Centre for Biotechnology Information (NCBI). (http://www.ncbi.nlm.nih.gov/) (accessed on OR603165).

Optimization of the selected fungal growth condition for the biosynthesis ZnO NPs

The optimization of ZnO NPs biosynthesis was done according to **Agarwal et al.** [73] and **Del Buono et al.** [74]. ZnO NPs biosynthesis response combinations were maintained with various parametric condition each independently, such as pH (4, 5, 6, 7 and 8), temp. (20, 25, 30, 35 and 40^{o}C), incubation period (1, 3, 5, 7 and 9 days), inoculum size (1, 2, 3, 4 and 5 discs of fungal mycelium) and zinc acetate concentration (1, 2, 3, 4

and 5mM). All ZnO NPs reaction mixtures were examined visually for color change and subjected to UV-visible spectrometry measurement (UV-1800; Shimadzu UV Spectrophotometer, Kyoto, Japan) to observe surface plasmon resonance signal (SPR) following 3 days of cultivation under the matching reaction-related circumstances, all with the exception of one parameter. Finally, each parametric condition was tested to exhibit the optimum antimicrobial activity against MDR *P. aeruginosa*.

Factorial experimental design for optimization of fungal biomass for ZnO NPS biosynthesis using Taguchi design

In this experiment, for the study of five factors; pH, temperature, incubation time, inoculum size, and precursor concentration, an L-25 (5^2) standard orthogonal arrays were created based on the results of manual optimization. The L-25 symbolic array of the experimental matrix represents the number of runs (i.e, 25 experimental trials) [75]. The antimicrobial activity of all 25 runs was studied to determine the optimized ZnO NPs conditions against MDR *P. aeruginosa* by the aforementioned procedures.

Minimum inhibitory concentration (MIC) of the most effective run for biosynthesis ZnO NPs

Two hundred micron of the tested bacterial suspension (2 x10^6 CFU/ ml) was inoculated on the nutrient agar plates. Different concentrations ZnO NPs using (1, 2, 3, 4, and 5mM) zinc acetate, and 250µl of each concentration were added to the agar wells. The plates were allowed to stand at 4^{o}C for 2h before incubation to allow the diffusion of the antimicrobial agent The plates were incubated for 24h at 37^{o}C. The antimicrobial activity of biosynthesis ZnO NPs was determined and the MIC was also measured by the growth diameter from the concentration of the lowest dosed well visually showing no growth [76].

Synthesized ZnO Nanoparticles (ZnONPs) Characterization

ZnO NPs were characterized by various conventional methods. The ultraviolet-visible (UV–Vis) spectrum of the ZnO NPs suspension was assessed using UV–Vis spectroscopy (UV-1800; Shimadzu UV Spectrophotometer, Kyoto, Japan), with a wavelength range of 200–800 nm at a resolution of 10nm [31]. Fourier transform infrared (FTIR) spectrum (Bruker α-T, Germany FT-IR spectrometer operating in the 400–4000 cm^{-1} range add city and name) for the functional group characterization that attached to ZnO NPs surface [77]. Transmission electron microscopy (TEM) was used to analyze the size distribution of the synthetic particles nanostructure using HITACHI H-800 (JEOL, Japan), operating at 200 kV [29]. To assess the zeta size and potential, a Malvern Zetasizer nanoseries compact scattering spectrometer and dynamic light scattering (Malvern Instruments Ltd., Malvern, UK) were employed, respectively at fixed angle of 173° at 25° C. Zetasizer software (version 7.11; Malvern Panalytical, Malvern, UK) created the histogram. Using Malvern's folded capillary cell, the zeta potential was determined [62]. ZnO NPs were examined using X-ray diffraction (XRD) to determine their crystalline structure. using a model Bruker (D8-DISCOVER)

diffractometer. Cu-Kα radiation of 1.54060A^{o} wavelength at 40k V and 30mA. The minerals of the core materials were identified using JCPDS carts, the relative intensity data were gathered over 2θ range of 5^{o}-100^{o}, 2θ values and relative intensities (1/1o) were calculated from the chart [78].

Cytotoxicity assay of ZnO NPs

The cytotoxicity potential of the biosynthesized ZnO NPs was studied against normal skin cell line Hfb4 and human breast carcinoma cell lines (MCF-7) compared with chemically synthesized ZnO NPs having a particle size of 50 nm and a surface area of more than 10.8 m^2/g were purchased from Sigma-Aldrich, Germany. Also, Antiviral activity of ZnO NPs against Herpes-simplex virus type-1 (HSV1) using MTT protocol according to **Riss and Moravec** [79].

In vitro, Efficacy against MDR P. aeruginosa

In vitro antibacterial activity of the biosynthesized ZnO NPs (MIC), chemically synthesized ZnO NPs, antibiotic fusidic acid (20mg/100ml) as a positive control, and zinc acetate in dist. H_2O, and dist. H_2O as a negative control was first put to the test using the agar diffusion technique aganist MDR *P. aeruginosa* strain. After 200 µl of freshly prepared bacterial suspension (2× 10^6 CFU/ ml) was separately added to each constructed well, a cork borer was used to make 6mm wells on the surface of nutrient agar plates [80]. The three replicates of the inhibitory zone diameter were measured in mm after the plates were incubated at 37°C overnight [81, 82].

In Vivo Pseudomonas aeruginosa Susceptibility for ZnO-NPs

The ability of biosynthesized ZnO NPs to fight MDR *P. aeruginosa in vivo* and promote wound healing was evaluated in an excision wound model in rats [83].

Experimental animal

A total number of 36 adult female Wister albino rats, weighing 200 ± 50gm, were housed at animal house, Faculty of Science (boys), Al-Azhar University, Cairo, Egypt. Nine rats/group were used for each treatment group, each rats group housed separately in polypropylene cages and maintained on a standard pellet diet and tap water under standard laboratory conditions of temperature 22-25^{o}C and subjected to light/dark cycles. Before beginning of the experiment, the animals were kept for 10 days for acclimatization. Through the experiment, all animals received humane care and this study was approved by the Ethics Committee of Science, Faculty of Women, Ain Shams University (Sci1232309001).
A total number of 36 adult female Wister albino rats, weighing 200 ± 50gm, were housed at animal house, Faculty of Science (boys), Al-Azhar University, Cairo, Egypt. Nine rats/group were used for each treatment group, each rats group housed separately in polypropylene cages and maintained on a standard pellet diet and tap water under standard laboratory conditions of temperature 22-25^{o}C and subjected to light/dark cycles. Before beginning of the experiment, the animals were kept for 10 days for acclimatization. Through

the experiment, all animals received humane care and this study was approved by the Ethics Committee of Science, Faculty of Women, Ain Shams University (Sci1232309001).

Experimental design

After one week of acclimatization, using hair clippers, the skin on the dorsal surfaces was removed. Using fine, sterilized scissors, a 1.5 x 1.5 cm^2 circular incision was created with caution [84]. Five minutes later, rat excision wounds were infected with *Pseudomonas aeruginosa* (n = 36) and inoculated with 200µl (approximately 2 $x10^6$ CFU/ml) of bacterial suspension then subdivided into 4 major groups: GIa (wounded, infected, and treated with saline), GIb (wounded, infected, and treated with fusidic acid (20mg/100ml), GIc (wounded, infected, and treated with the biosynthesized ZnO NPs) and GId (wounded, infected, and treated with the chemical ZnO NPs). After appearance of lesions and pus cells, all groups received 250µl of each treatment three times daily. Also, 6 rats were involved in the study: GII (n = 3) as a healthy control and GIII (n = 3) (wounded, uninfected, and untreated) as a negative control.

Determination of wound healing efficiency

Sample collection and preparation

On the tenth day following the wound, by carefully removing a suitable and consistent amount of the surrounding wound margin using sterile scissors, rat wound tissue samples were meticulously cut from the healing skin of rats in all groups. To fully remove the granulation tissue from the healing wound, deep cuts were performed into the underlying tissue. The samples from the wounds were frozen and stored in -80^oC. Prior to analysis, wound samples were centrifuged for 15 minutes at 12000 rpm in phosphate buffered saline (PBS, PH 7.4) ice-cold, the supernatant was collected and kept at -80^oC. These samples were utilized to conduct biochemical analyses of lipid peroxidation (LPO) and inflammations, which are both caused by endogenous antioxidant enzyme activities.

Tissue analysis by colorimetric method

Measurement of Lipid peroxidation level (LPO)

Malondialdehyde (MDA) was used to express the amount of lipid peroxidation in tissue samples. It was measured using the method of **Ohkawa et al.** [85].

Estimation of Superoxide dismutase (SOD)

Superoxide dismutase was determined spectrophotometrically at 560 nm according to the method of **Nishikimi et al.** [86].

Measurement of cytokines concentration

The Tumor Necrosis Factor Alpha (TNFα) and Interleukin 1 Beta (IL1β) concentrations in the samples was measured using an enzyme linked immune sorbent assay (ELISA) kit [87].

Histopathological studies

For general histological examination, sections with 6µm in thickness were harvested from central portion of the wound according to the standard method by **Harris** [88]. Tissue sections were fixed in a 10% buffered formalin, then dehydrated with an ethanol series starting at 70% and ending with an absolute, paraffin-embedded section. After staining with hematoxylin- eosin (H&E) the sections were examined using an electric light microscope (Olympus BX43) and captured using Olympus DP27 camera linked to CellSens dimensions software (Olympus).

Statistical analysis.

This study's statistical analysis was conducted using SPSS 28, sigma plot and excel version 2007. Three replicates of each outcome were recorded. Mean, standard deviation and standard error were determined [89]. Optimization was made using Taguchi experimental design by minitab program version 17.

Declarations

Acknowledgements

The authors would like to thank Dr. Marwa Tarek Ebrahim Assistant professor of histology and histochemistry, Zoology Department, Faculty of Women for Arts, Science and Education, Ain Shams University for her kindly help in interpretation of soft tissue wound histology

Author contributions

Z.M.H.K. and M.A.H. conceived and designed the study; H.R.M., Salah Abdelbary and E.E.M. performed the experiments; E.E.M. drafted the manuscript; Z.M.H.K., E.E.M and H.R.M. interpreted the experimental results; Z.M.H.K. and M.A.H. revised the manuscript. All authors have read and agreed to the published version of the manuscript.

Data Availability

All data generated and analyzed during the current study are available from the corresponding author on reasonable request.

Ethics approval

The Ethics approval is obtained from the Ethics Committee of Faculty of Women for Art, Science and Education, Ain Shams University (Sci1232309001).

Consent for publication

Not applicable.

Declaration of competing interest

The authors declare no known competing financial interests or personal.

Funding

This study doesn’t receive any fund.

References

1. Kolar M, Urbanek K, Latal T. Antibiotic selective pressure and development of bacterial resistance. *Int J Antimicrob Ag*. 2001; 17: 357-363.
2. Saffle JR, Davis B, Williams P. Recent outcomes in the treatment of burn injury in the United States: a report from the American Burn Association Patient Registry. J Burn Care Rehabil 1995; 16: 219-232.
3. Church D, Elsayed S, Reid O, Winston B, Lindsay R. Burn wound infections. *Clin Microbiol Rev*. 2006;19(2):403-434.
4. Ghasemian S, Karami-Zarandi M, Heidari H, Khoshnood S, Kouhsari E, Ghafourian S, Kazemian H. Molecular characterizations of antibiotic resistance, biofilm formation, and virulence determinants of Pseudomonas aeruginosa isolated from burn wound infection. *Journal of Clinical Laboratory Analysis*. 2023; *7*(4), e24850.
5. Edwards-Jones V, Greenwood JE. Manchester Burns Research Group (2003) What's new in burn microbiology? James Laing Memorial Prize Essay 2000. Burns 29: 15-24.
6. Gallagher JJ, Williams-Bouyer N, Villarreal C, Heggers JP, Herndon DN (2007) Treatment of infection in burns. Total Burn Care, (3rdedtn), In: Herndon DN. Philadelphia: WB Saunders, 136-176.
7. Magiorakos AP, Srinivasan A, Carey RB, Carmeli Y, Falagas ME. Multidrug-resistant, extensively drug-resistant and pandrugresistant bacteria: an international expert proposal for interim standard definitions for acquired resistance. Clin Microbiol Infect. 2012; 18:268-281.
8. Afifi M, Almaghrabi O A, and Kadasa N M (2015). Ameliorative Effect of Zinc Oxide Nanoparticles on Antioxidants and Sperm Characteristics in Streptozotocin-Induced Diabetic Rat Testes. BioMed. Res. Int. 2015; 2015. Article ID 153573, 6 pages. doi: 10.1155/2015/153573.
9. Chandrasekaran R, Gnanasekar S, Seetharaman P, Keppanan R, Arockiaswamy W and Sivaperumal S. Formulation of Carica Papaya Latex-Functionalized Silver Nanoparticles for Its Improved Antibacterial and Anticancer Applications. J. Mol. Liq. 2016; 219: 232–238. doi: 10.1016/j.molliq.2016.03.038.
10. Castro-Aceituno V, Ahn S, Simu S Y, Singh P, Mathiyalagan R and Lee H A. (2016). Anticancer Activity of Silver Nanoparticles From Panax Ginseng Fresh Leaves in Human Cancer Cells. Biomed. Pharmacother. 2016; 84:158-165. doi: 10.1016/ j.biopha.2016.09.016.

11. Sastry M, Ahmad A, Khan I and Kumar R. Biosynthesis of metal nanoparticles using fungi and actinomycete. Curr. Sci.2003; 85 (2):162-70.
12. Castro-Longoria E, Vilchis-Nestor AR, and Avalos-Borja M. Biosynthesis of Silver, Gold and Bimetallic Nanoparticles Using the Filamentous Fungus Neurospora Crassa. Colloids Surfaces B Biointerfaces. 2011; 83: 42–48. doi: 10.1016/j.colsurfb.2010.10.035.
13. Gunalan S, Sivaraj R and Rajendran V. Green synthesized ZnO nanoparticles against bacterial and fungal pathogens. Progress in Nat. Sci., Materials Int.,2012; 22 (6): 693-700.
14. Pati R, Mehta RK, Mohanty S, Padhi A, Sengupta M and Vaseeharan B. Topical application of zinc oxide nanoparticles reduces bacterial skin infection in mice and exhibits antibacterial activity by inducing oxidative stress response and cell membrane disintegration in macrophages. Nanomedicine. 2014; 10(6): 1195-208.
15. Khan Z U H, Sadiq H M, Shah N S, Khan A U, Muhammad N, Hassan S U, Tahir K, Khan F U, Imran M, Ahmad N, Shafi S, Ullah F, Ahmad A, Sayed M, Khalid M, Qaisrani S, Ali M and Zakir A. Greener Synthesis of zinc oxide nanoparticles using *Trianthema portulacastrum* extract and evaluation of its photocatalytic and biological applications. Journal of Photochemistry and Photobiology B: Biology. . 2019; 192:147–157. Doi:10.1016/j.jphotobiol.2019.01.013.
16. Kalpana V N, Kataru B A S, Sravani N, Vigneshwari T, Panneerselvam A and Rajeswari V D. Biosynthesis of zinc oxide nanoparticles using culture filtrates of *Aspergillus niger*: Antimicrobial textiles and dye degradation studies. Open Nano. 2018; 3(2018):48–55. https://doi.org/10.1016/j.onano.2018.06.001.
17. Shamim A, Abid M B and Mahmood T. Biogenic Synthesis of Zinc Oxide (ZnO) Nanoparticles Using a Fungus (*Aspargillus niger)* and Their Characterization. International Journal of Chemistry.2019; 11(2): 119-126. doi:10.5539/ijc.v11n2p119.
18. Sreenivas R R, Prakasham R S, Krishna P K, Rajesham S, Sharma P N and Venkateswar R L. Xylitol production by Candida sp.: parameter optimization using Taguchi approach. Process Biochemistry. 2004; 39: 951-956.
19. Sivarao S, Anand T and Ammar A. DOE based statistical approaches in modeling of laser processing-review and suggestion. International Journal of Engineering and Technology.2010; 10: 1-8.
20. Mekky A E, Farrag A A, Hmed A A and Sofy A R. Preparation of Zinc Oxide Nanoparticles using *Aspergillus niger* as Antimicrobial and Anticancer Agents. Journal of Pure and Applied Microbiology. 2021; 15(3):1547- 1566. https://doi.org/10.22207/JPAM.15.3.49.
21. Shah M, Fawcett D, Sharma S, Tripathy S K and Poinern G E J. Green synthesis of metallic nanoparticles via biological entities. Materials. 2015; 8 (11): 7278-7308. https://doi.org/10.3390/ma8115377.
22. Hassani S M, Nakhaei M M and Forghanifard M.M. Inhibitory effect of zinc oxide nanoparticles on *pseudomonas aeruginosa* biofilm formation. Nanomedicine Journal. 2015; 2 (2): 121-128.
23. Dobrucka R and Długaszewska J. Biosynthesis and antibacterial activity of ZnO nanoparticles using *Trifolium pratense* flower extract. Saudi Journal of Biological Sciences. 2016**;** 23 (4): 517-523. https://doi.org/10.1016/j.sjbs.2015.05.016

24. Rajeshkumar S. Synthesis of silver nanoparticles using fresh bark of *Pongamia pinnata* and characterization of its antibacterial activity against gram positive and gram negative pathogens. Resource-Efficient Technologies. 2016; 2 (1): 30- 35. https://doi.org/10.1016/j.reffit.2016.06.003.
25. El-Rafie M H, Mohamed A A, Shaheen T I and Hebeish A. Antimicrobial effect of silver nanoparticles produced by fungal process on cotton fabrics, Carbohydrate Polymers. 2010; 80 (3): 779-782. https://doi.org/10.1016/j.carbpol.2009.12.028.
26. Gupta P, Bajpai M and Bajpai S K. Investigation of antibacterial properties of silver nanoparticle loaded poly (acrylamide-co-itaconic acid)-grafted cotton fabric. Journal of Cotton Science. 2008; 12: 280–286. http://journal.cotton.org.
27. Khan S A, Noreen F, Kanwal S, Iqbal A and Hussain G. Green synthesis of ZnO and Cu-doped ZnO nanoparticles from leaf extracts of *Abutilon indicum*, *Clerodendrum infortunatum*, *Clerodendrum inerme* and investigation of their biological and photocatalytic activities. Materials Science and Engineering: C. 2018; 82 (2018): 46-59. https://doi.org/10.1016/j.msec.2017.08.071
28. Manke A, Wang L and Rojanasakul Y. Mechanisms of nanoparticle-induced oxidative stress and toxicity, BioMed research international, 2013; 2013; 1-15. (Article ID 942916) http://dx.doi.org/10.1155/2013/942916
29. Hefny ME, El-Zamek FI, El-Fattah A and Mahgoub SAM. Biosynthesis of Zinc Nanoparticles Using Culture Filtrates of *Aspergillus, Fusarium And Penicillium* Fungal Species And Their Antibacterial Properties Against Gram-Positive And Gram-Negative Bacteria. Zagazig Journal of Agricultural Research. 2019; 46 (6A): 2009-2021. DOI: 10.21608/zjar.2019.51920.
30. Es-haghi A, Taghavizadeh Yazdi M E, Sharifalhoseini M, Baghani M, Yousefi E, Rahdar A and Baino F. Application of Response Surface Methodology for Optimizing the Therapeutic Activity of ZnO Nanoparticles Biosynthesized from *Aspergillus niger*. Biomimetics. 2020; 6 (2): 1-13 https://doi.org/10.3390/biomimetics6020034.
31. Rasha E, Alkhulaifi M M, AlOthman M, Khalid I, Doaa E, Alaa K, Awad M A and Abdalla M. Effects of Zinc Oxide Nanoparticles Synthesized Using *Aspergillus niger* on Carbapenem-Resistant *Klebsiella pneumonia In Vitro* and *In Vivo*. Frontiers in Cellular and Infection Microbiology. 2021a: 11 (748739). Doi:10.3389/fcimb.2021.748739.
32. Kalaba M H, Moghannem S A, El-Hawary A S, Radwan A A, Sharaf M H and Shaban A S. Green Synthesized ZnO Nanoparticles Mediated by *Streptomyces plicatus*: Characterizations, Antimicrobial and Nematicidal Activities and Cytogenetic Effects. Plants. 2021; 10(9): 1-26. https://doi.org/10.3390/plants10091760.
33. Chen C, Yu B, Liu P, Liu J and Wang L. Investigation of nano-sized ZnO particles fabricated by various synthesis routes. Journal of ceramic processing research. 2011; 12 (4): 420– 425.
34. Ashwini J, Aswathy TR, Rahul A B, Thara G M and Nair A S. Synthesis and Characterization of Zinc Oxide Nanoparticles Using *Acacia caesia* Bark Extract and Its Photocatalytic and Antimicrobial Activities. Catalysts. 2021; 11 (12) 1-20. https://doi.org/10.3390/catal11121507.
35. Abdelmigid H M, Hussien N A, Alyamani A A, Morsi M M, AlSufyani N M and Kadi H A. Green Synthesis of Zinc Oxide Nanoparticles Using Pomegranate Fruit Peel and Solid Coffee Grounds vs. Chemical

Method of Synthesis, with Their Biocompatibility and Antibacterial Properties Investigation. Molecules. 2022; 27 (4): 1- 17. https:// doi.org/10.3390/molecules27041236.

36. Gao Y, Anand M A V, Ramachandran V, Karthikkumar V, Shalini V, Vijayalakshmi S and Ernest D Biofabrication of zinc oxide nanoparticles from *Aspergillus niger*, their antioxidant, antimicrobial and anticancer activity. Journal of Cluster Science. 2019; 30: 937–946. https://doi.org/10.1007/ s10876-019-01551-6.
37. Vimala K, Sundarraj S, Paulpandi M, Vengatesan S and Kannan S. Green synthesized doxorubicin loaded zinc oxide nanoparticles regulates the Bax and Bcl-2 expression in breast and colon carcinoma. Process Biochemistry. 2014; 49 (1): 160– 172. https://doi.org/10.1016/j.procbio.2013.10.007
38. Jan H, Shah M, Usman H, Khan M A, Zia M, Hano C and Abbasi B H. Biogenic Synthesis and Characterization of Antimicrobial and Antiparasitic Zinc Oxide (ZnO) Nanoparticles Using Aqueous Extracts of the Himalayan Columbine (*Aquilegia pubiflora).* Frontiers in Materials. 2020; 7(249): 1-14. https://doi.org/10.3389/fmats.2020.00249.
39. Manosalva N, Tortella G, Cristina Diez M, Schalchli H, Seabra A B, Durán N and Rubilar O. Green synthesis of silver nanoparticles: Effect of synthesis reaction parameters on antimicrobial activity. World Journal of Microbiology and Biotechnology; 2019; 35(88): 1-9. https://doi.org/10.1007/s11274-019-2664-3.
40. Senthilraja P and Kathiresan K. *In vitro* cytotoxicity MTT assay in Vero, HepG2 and MCF-7 cell lines study of marine yeast. Journal of Applied Pharmaceutical Science. 2015; 5 (03):080– 084. DOI: 10.7324/JAPS.2015.50313.
41. Sayed H M, Said M M, Morcos N YS, El Gawish M A and Ismail A F M. Antitumor and Radiosensitizing Effects of Zinc Oxide-Caffeic Acid Nanoparticles against Solid Ehrlich Carcinoma in Female Mice. Integrative Cancer Therapies. 2021; 20: 1–22. https://doi.org/10.1177/15347354211021920.
42. Ruddaraju L K, Pammi S V N, Pallela P V K, Padavala V S and Kolapalli V R M. Antibiotic potentiation and anti-cancer competence through bio-mediated ZnO nanoparticles. Materials Science and Engineering: C. 2019; 103 (2019): 1-11. https://doi.org/10.1016/j.msec.2019.109756.
43. Padalia H and Chanda S. Characterization, antifungal and cytotoxic evaluation of green synthesized zinc oxide nanoparticles using *Ziziphus nummularia* leaf extract. Artificial Cells, Nanomedicine, and Biotechnology. 2017; 45 (8): 1751–1761. https://doi.org/10.1080/21691401.2017.1282868.
44. Gomathi R Suhana H and Paradesi D. Characterization Study of Cytotoxicity of Green Synthesized ZnO Nanoparticles Loaded with Anti-Cancer Doxorubicin Drug. Chemistry Select. 2021; 6 (18):4533– 4538. https://doi.org/10.1002/slct.202100358.
45. Shen C, James S A, de Jonge M D, Turney T W, Wright P F and Feltis B N. Relating cytotoxicity, zinc ions, and reactive oxygen in ZnO nanoparticle–exposed human immune cells. Toxicological Sciences. 2013; 136 (1): 120– 130. https://doi.org/10.1093/toxsci/kft187.
46. Scherzad A, Meyer T, Kleinsasser N and Hackenberg S. Molecular mechanisms of zinc oxide nanoparticle-induced genotoxicity. Materials. 2017; 10 (12, 1427): 1-19. https://doi.org/10.3390/ma10121427.

47. Ishida T. Anti-viral vaccine activity of Zinc (II) for viral prevention, entry, replication, and spreading during pathogenesis process. Current Trends in Biomedical Engineering & Biosciences. 2019; 19 (3, 556012): 0083– 0088. DOI: 10.19080/CTBEB.2019.19.556012.
48. Gurunathan S, Qasim M, Choi Y, Do J T, Park C, Hong K, Kim J H and Song H. Antiviral potential of nanoparticles—can nanoparticles fight against coronaviruses? Nanomaterials. 2020; 10 (9):1- 29.
49. Tavakoli A, Ataei-Pirkooh A, Sadeghi G M M, Bokharaei-Salim F, Sahrapour P, Kiani S J, Moghoofei M, Farahmand M, Javanmard D and Monavari S H. Polyethylene glycol-coated zinc oxide nanoparticle: An efficient nanoweapon to fight against herpes simplex virus type 1. Nanomedicine. 2018; 13 (21): 2675–2690. https://doi.org/10.2217/nnm-2018-0089.
50. Ghaffari H, Tavakoli A, Moradi A, Tabarraei A, Bokharaei-Salim F, Zahmatkeshan M, Farahmand M, Javanmard D, Kiani S, Esghaei M, Pirhajati V, Ataei-Pirkooh A and Monavari S. Inhibition of H1N1 influenza virus infection by zinc oxide nanoparticles: Another emerging application of nanomedicine. Journal of Biomedical Science. 2019; 26 (70):1-10. https://doi.org/10.1186/s12929- 019- 0563- 4.
51. El-Megharbel S M, Alsawat M, Al-Salmi F A and Hamza R Z. Utilizing of (zinc oxide nano-spray) for disinfection against “SARS-CoV-2” and testing its biological effectiveness on some biochemical parameters during (COVID-19 pandemic)—” ZnO nanoparticles have antiviral activity against (SARS-CoV-2). Coatings. 2021; 11(4, 388): 1-14. Doi: 10.3390/coatings11040388.
52. Kelly S A, Havrilla C M, Brady T C, Abramo K H and Levin E D. Oxidative stress in toxicology: established mammalian and emerging piscine model systems. Environmental Health Perspectives; 1998; 106 (7):375– 384. https://doi.org/10.1289/ehp.98106375.
53. Siddiqi K S, ur Rahman A, Tajuddin and Husen A. Properties of Zinc Oxide Nanoparticles and Their Activity against Microbes. Nanoscale Research Letters. 2018; 13 (141): 1-13. https://doi.org/10.1186/s11671-018-2532-3.
54. Prasad A S. Clinical, immunological, anti-inflammatory and antioxidant roles of zinc. Experimental Gerontology. 2008; 43(5): 370– 377. https://doi.org/10.1016/j.exger.2007.10.013.
55. Abd El-Hack M E, Alagawany M, Salah A S, Abdel-Latif M A and Farghly M FA. Effects of dietary supplementation of zinc oxide and zinc methionine on layer performance, egg quality, and blood serum indices. Biological Trace Element Research, 2018b; 184 (2): 456– 462. https://doi.org/10.1007/s12011-017-1190-0.
56. Nishikimi M, Roa N A and Yogi K. The Occurrence of Supeoxide Anion in the Reaction of Reduced Phenazine Methosulfate and Molecular Oxygen. Biochemical and Biophysical Research Communications. 1972; 46 (2): 849- 854.
57. Tang H Q, Xu M, Rong Q, Jin R W, Liu Q J and Li Y L. The effect of ZnO nanoparticles on liver function in rats. International Journal of Nanomedicine. 2016; (11):4275-4285. doi: 10.2147/IJN.S109031.
58. Li J, Chen H, Wang B, Cai C, Yang X, Chai Z and Feng W. ZnO nanoparticles act as supportive therapy in DSS-induced ulcerative colitis in mice by maintaining gut homeostasis and activating Nrf2 signaling. Scientific Reports. 2017; 7: (43126): 1-11. DOI: https://doi.org/10.1038/srep43126.
59. Abass M A, Selim S A, Selim A O, El-Shal A S and Gouda Z A. Effect of orally administered zinc oxide nanoparticles on albino rat thymus and spleen. IUBMB Life. 2017; 69 (7): 528-539.

https://doi.org/10.1002/iub.1638.

60. Roy R, Kumar S, Verma A K, Sharma A, Chaudhari B P, Tripathi A and Dwivedi D M. Zinc nanoparticles provide an adjuvant effect to ovalbumin via Th2 response in Balb /c mice. International Immunology. 2014; 26 (3): 159-172. https://doi.org/10.1093/intimm/dxt053.
61. Mobarez E, Azoz H, Alkalamawy N, Nada A, Ibraheem E M, Jaber M Z and Taha H S. Evaluation the Effectiveness of Green Zinc Oxide Nanoparticles on the Anti-Inflammatory Effect of Dexamethasone and Its Side Effects in Rats. SVU-International Journal of Veterinary Sciences. 2018; 1 (1): 25-54. DOI: 10.21608/SVU.2018.17924.
62. Rasha E, Monerah, A, Manal A, Rehab A, Mohammed D and Doaa E. Biosynthesis of Zinc Oxide Nanoparticles from *Acacia nilotica* (L.) Extract to Overcome Carbapenem-Resistant *Klebsiella Pneumoniae*. Molecules. 2021b; 26 (7):1919. https://doi.org/10.3390/molecules26071919.
63. Gao Y, Han Y, Cui M, Tey H L, Wang L and Xu C. ZnO nanoparticles as an antimicrobial tissue adhesive for skin wound closure. Journal of Materials Chemistry B. 2017; 5: 4535– 4541. DOI: 10.1039/c7tb00664k.
64. Rao T N, Riyazuddin; Babji, P, Ahmad N, Khan R A, Hassan I, Shahzad S A and Husain F M. Green synthesis and structural classification of *Acacia nilotica* mediated-silver doped titanium oxide (Ag/TiO2) spherical nanoparticles: Assessment of its antimicrobial and anticancer activity. Saudi Journal of Biological Sciences. 2019; 26 (7): 1385- 1391. https://doi.org/10.1016/j.sjbs.2019.09.00
65. Howida RM, Zeinab MHK, Maha A H, Ayman F A, Elam EE, Salah Abdelbary. Trends in the assessment of multidrug efficiency against identified bacterial strains isolated from wounds at El-Demerdash Hospital, Egypt. Journal of Scientific Research in Science 2022; 39, (2): 82-101.
66. Waksman S A 1927. Principles of Soil Microbiology, Williams and Wilkins Co. Baltimore, Md. Agronomy Journal, 1927; 20 (11): 1- 654. https://doi.org/10.2134/agronj1928.00021962002000110014x
67. Raja M, Praveena G and WilliamS J. Isolation and Identification of fungi from soil in Loyola College Campus, Chennai, India. International Journal of Current Microbiology and Applied Sciences,2017; 6 (2):1789-1795. DOI:10.20546/ijcmas.2017.602.200.
68. Jain N, Bhargava A, Majumdar S, Tarafdar J C, and Panwar J. Extracellular biosynthesis and characterization of silver nanoparticles using *Aspergillus flavus* NJP08: a mechanism perspective. Nanoscale, 2011; 3: 635–641.
69. Mohd Yusof H, Abdul Rahman N, Mohamad R, Zaidan UH and Samsudin AA. Biosynthesis of zinc oxide nanoparticles by cell-biomass and supernatant of *Lactobacillus plantarum* TA4 and its antibacterial and biocompatibility properties. Scientific Reports, 2020; 10 (19996):1-13. https://doi.org/10.1038/s41598-020-76402-w.
70. Gupta M, Tomar R S, Kaushik S, Mishra R K and Sharma D. Effective Antimicrobial Activity of Green ZnO Nano Particles of *Catharanthus roseus*. Frontiers in Microbiology. 2018; 9 (2030):1-13. Doi:10.3389/fmicb.2018.02030.
71. Raper K B and Fennell D I. The Genus Aspergillus. Williams and Wilkins, Philadelphia, 1965; 686 p.
72. Diba K, Kordbacheh P, Mirhendi S H, Rezaie S and Mahmoudi M. Identification of aspergillus species using morphological characteristics. Pakistan Journal of Medical Sciences, (Part-II).2007; 23 (6): 867-

872.

73. Agarwal H, Venkat Kumar S and Rajeshkumar S. A review on green synthesis of zinc oxide nanoparticles An eco-friendly approach. Resource-Efficient Technologies. 2017; 3(4):406–413. https://doi.org/10.1016/j.reffit.2017.03.002
74. Del Buono D, Di Michele A, Costantino F, Trevisan M and Lucini L. Biogenic ZnO nanoparticles synthesized using a novel plant extract: Application to enhance physiological and biochemical traits in maize. Nanomaterials. 2021; 11(5, 1270):1-15. https://doi.org/10.3390/nano11051270
75. Hamzaçebi C. Taguchi Method as a Robust Design Tool. IntechOpen, 2020; 1-19. DOI: http://dx.doi.org/10.5772/intechopen.94908.
76. Housseiny M M and Gomaa E Z. Enhancement of Antimicrobial and Antitumor Activities of Zinc Nanoparticles Biosynthesized by *Penicillium chrysogenum* AUMC 10608 Using Gamma Radiation. Egyptian Journal of Botany,2019; 59 (2):319–337. DOI:10.21608/ejbo.2019.5492.1223.
77. Rajan A, Cherian E and Baskar G. Biosynthesis of zinc oxide nanoparticles using *Aspergillus fumigatus* JCF and its antibacterial activity. International Journal of Modern Science and Technology. 2016; 1(2):52-57.
78. Ismail M A, Taha K K, Modwi A and Khezami L. ZnO nanoparticles: surface and x-ray profile analysis. Journal of Ovonic Research. 2018; 14 (5): 381 – 393. https://www.researchgate.net/publication/328026905
79. Riss T L and Moravec R A. Use of Multiple Assay Endpoints to Investigate the Effects of Incubation Time, Dose of Toxin, and Plating Density in Cell-Based Cytotoxicity Assays. Assay and Drug Development Technologies, 2004; 2(1): 51-62. https://doi.org/10.1089/154065804322966315.
80. 80. Saddik M S, Elsayed M M A, El-Mokhtar M A, Sedky H, Abdel-Aleem J A, Abu-Dief A M, Al-Hakkani M F, Hussein H L, Al-Shelkamy S A, Meligy FY, Khames A and Abou-Taleb H A. Tailoring of Novel Azithromycin-Loaded Zinc Oxide Nanoparticles for Wound Healing. Pharmaceutics. 2022;14 (1,111): 1-23. https://doi.org/ 10.3390/pharmaceutics14010111.
81. Allam A, El-Mokhtar M A and Elsabahy M. Vancomycin-loaded niosomes integrated within pH-sensitive in-situ forming gel for treatment of ocular infections while minimizing drug irritation. Journal of Pharmacy and Pharmacology. 2019; 71(8):1209-1221. Doi: 10.1111/jphp.13106.
82. Hetta H F, Al-Kadmy I M S, Khazaal S S, Abbas S, Suhail A, El-Mokhtar M A, Ellah N H A, Ahmed E A, Abd-Ellatief R B, El-Masry E A, Batiha G E, Elkady A A, Mohamed N A and Algammal AM. Antibiofilm and antivirulence potential of silver nanoparticles against multidrug-resistant *Acinetobacter baumannii.* Scientifc Reports. 2021; 11(10751): 1-11. | https://doi.org/10.1038/s41598-021-90208-4.
83. Mekkawy A I, El-Mokhtar M A, Nafady N A, Yousef N, Hamad M A, El-Shanawany S M, Ibrahim E H and Elsabahy M. *In vitro* and *in vivo* evaluation of biologically synthesized silver nanoparticles for topical applications: Effect of surface coating and loading into hydrogels. International Journal of Nanomedicine. 2017; 12: 759-777. Doi: 10.2147/IJN.S124294.
84. Abd El-Hack M E, Alagawany M, Amer S A, Arif M, Wahdan K M and El-Kholy M S. Effect of dietary supplementation of organic zinc on laying performance, egg quality and some biochemical parameters

of laying hens. Journal of Animal Physiology and Animal Nutrition. 2018a: 102 (2): e542– e549. https://doi.org/10.1111/jpn.12793.

85. Ohkawa H, Ohishi Wand Yagi K. Assay for lipid peroxides in animal tissues by thiobarbituric acid reaction. Analytical Biochemistry. 1979; 95(2): 351- 358. DOI: 10.1016/0003-2697(79)90738-3.
86. Nishikimi M, Roa N A and Yogi K. The Occurrence of Supeoxide Anion in the Reaction of Reduced Phenazine Methosulfate and Molecular Oxygen. Biochemical and Biophysical Research Communications. 1972; 46 (2): 849- 854.
87. Kimura H, Suzui M, Nagao F and Matsumoto K. Highly Sensitive Determination of Plasma Cytokines by Time-Resolved Fluoroimmunoassay; Effect of Bicycle Exercise on Plasma Level of Interleukin-1α (IL-1. α), Tumor Necrosis Factor α (TNFα) and Interferon γ (IFN γ). Analytical Sciences. 2001; 17 (5): 593-597.
88. Harris H F. On the rapid conversion of haematoxylin into haematin staining reactions. Journal of Applied Microscopy and Laboratory Methods. 1900; 3, 777.
89. Lee D K, In J and Lee S. Standard deviation and standard error of the mean. Korean Journal of Anesthesiology.2015; 68 (3): 220-223. DOI: https://doi.org/10.4097/kjae.2015.68.3.220.

Figures

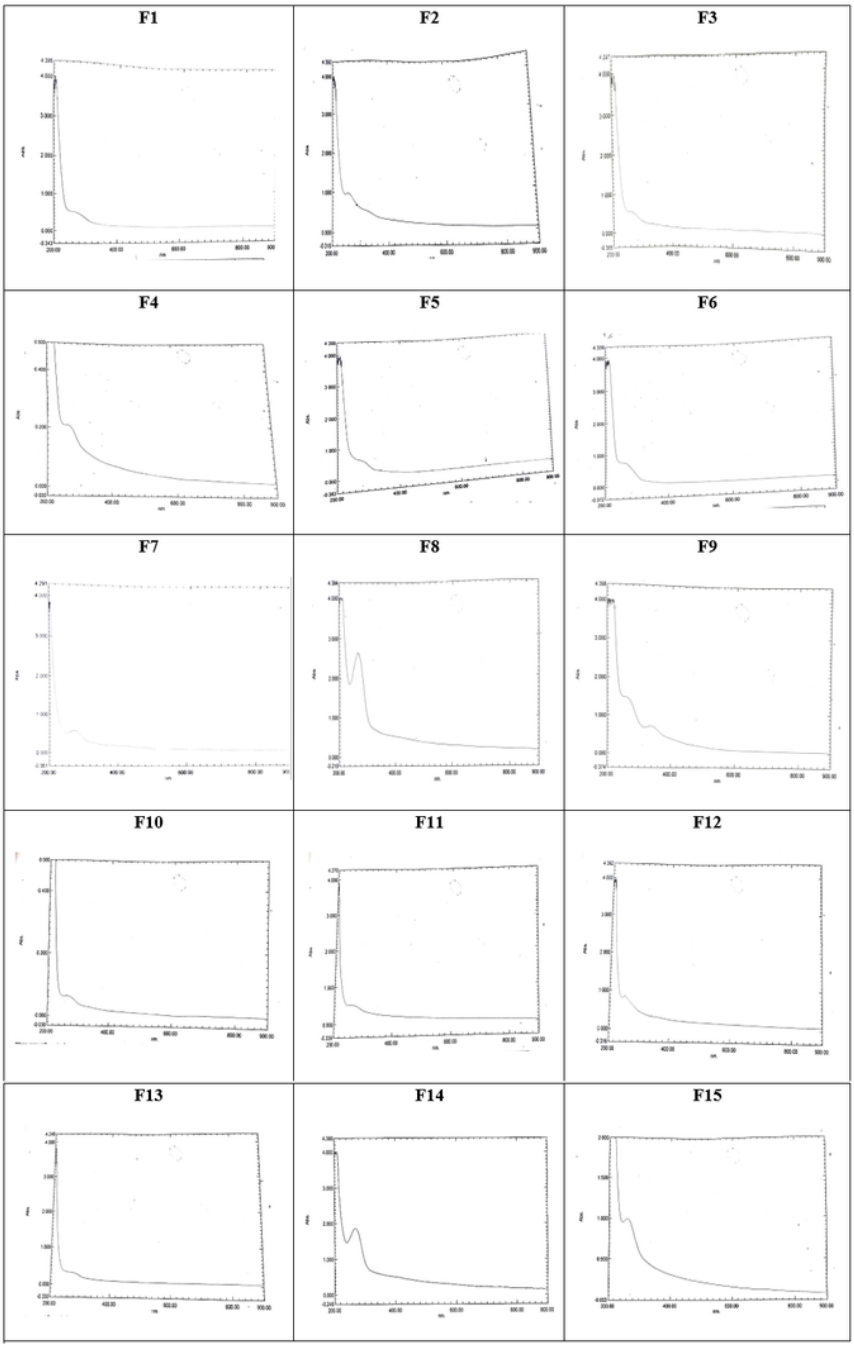

Figure 1

UV- spectroscopy of the biosynthesized ZnO NPs by the isolated fungi.

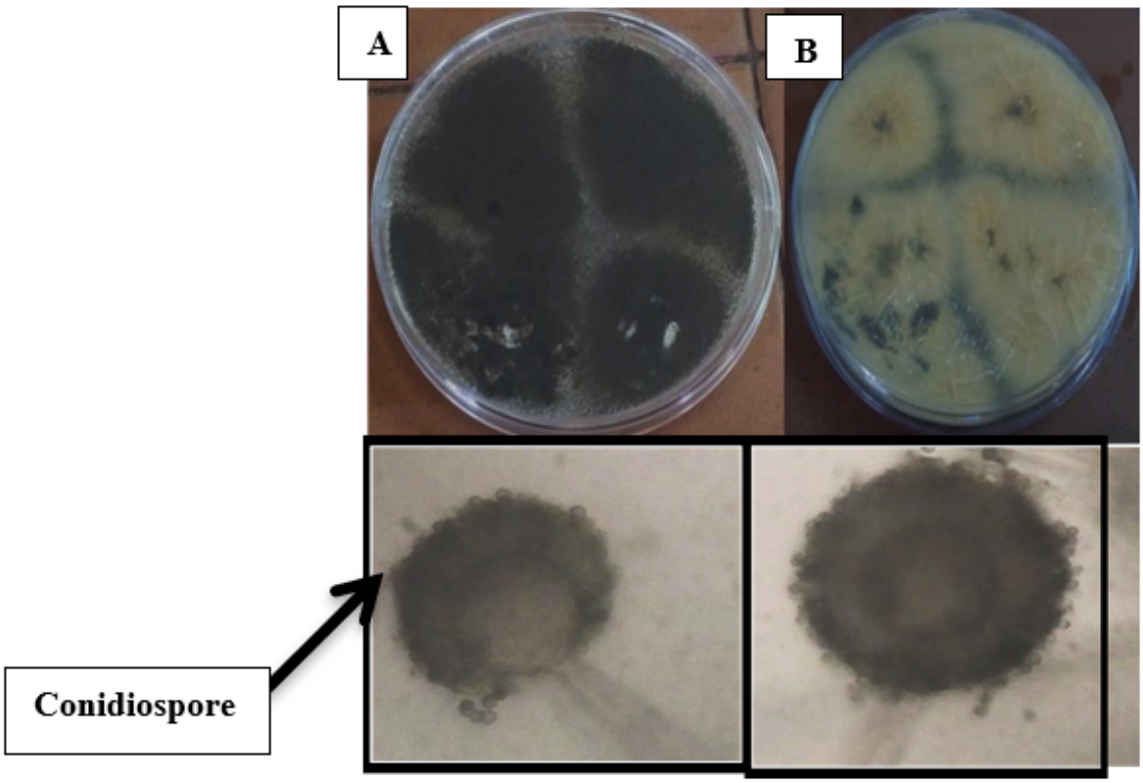

Figure 2

The morphological characteristics of a powerful fungus for biosynthesis of ZnO NPs where A; forward side and B; reverse side

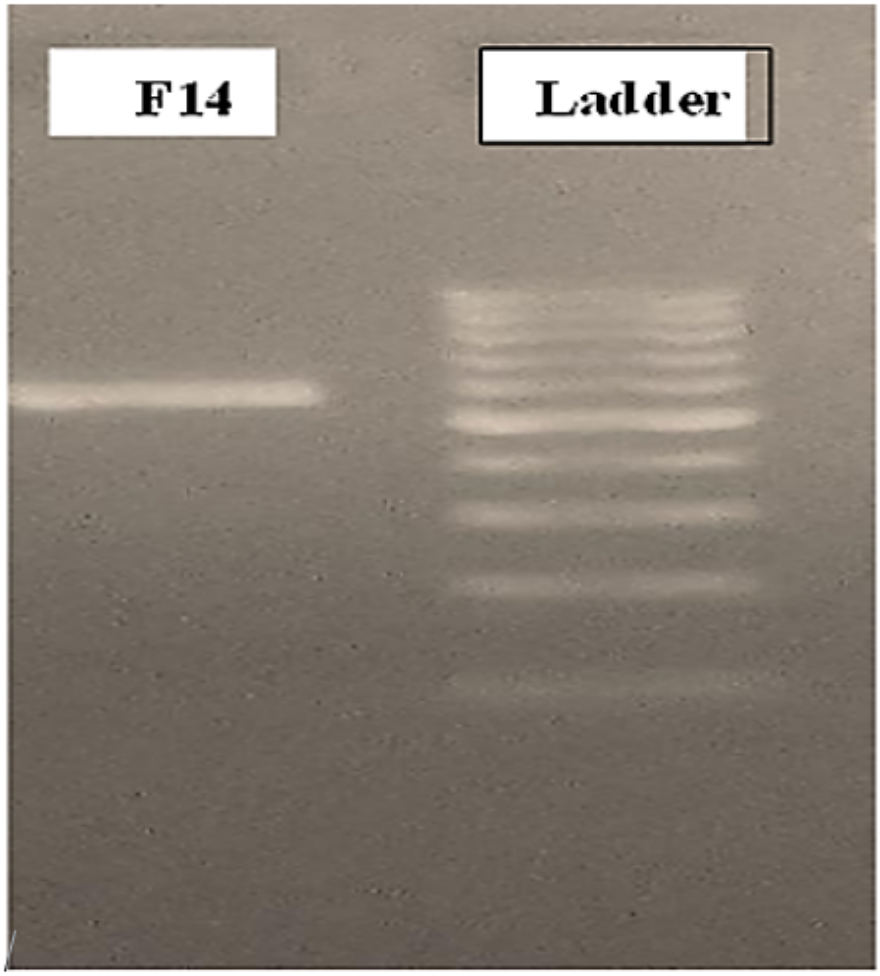

Figure 3

Gel electrophoresis of the most potent fungal isolate F14

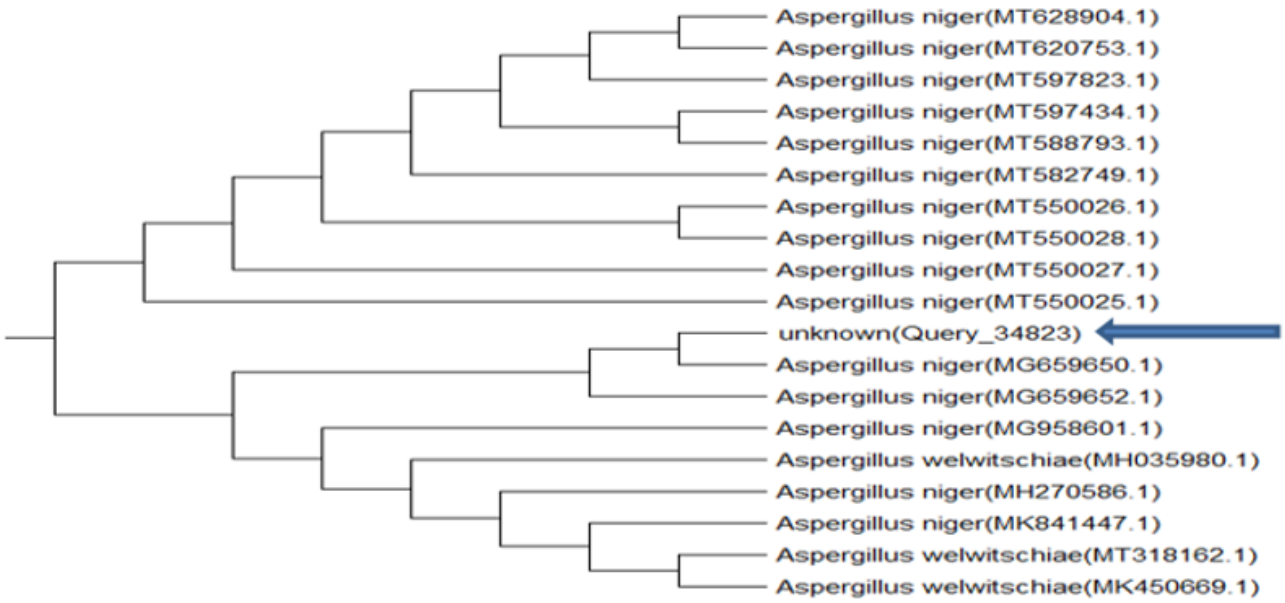

Figure 4

Phylogenetic tree created using the 18s rDNA sequencing of the fungus isolate code F14, related to *Aspergillus niger* with accession number OR603165.

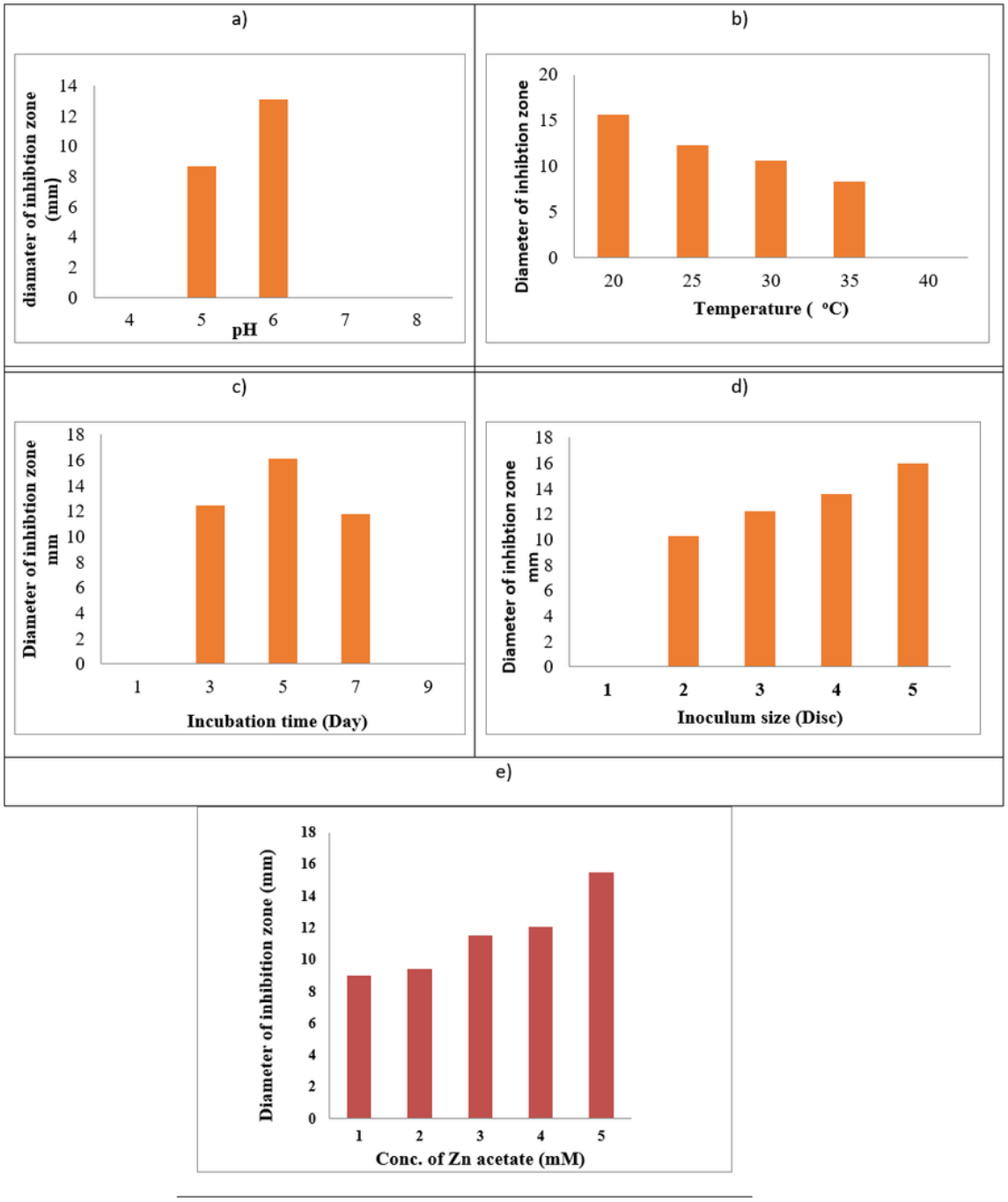

Figure 5

Effect of *A. niger* growth conditions on the antimicrobial activity of the biosynthesized of ZnO NPs against MDR *P. aeruginosa strain.*

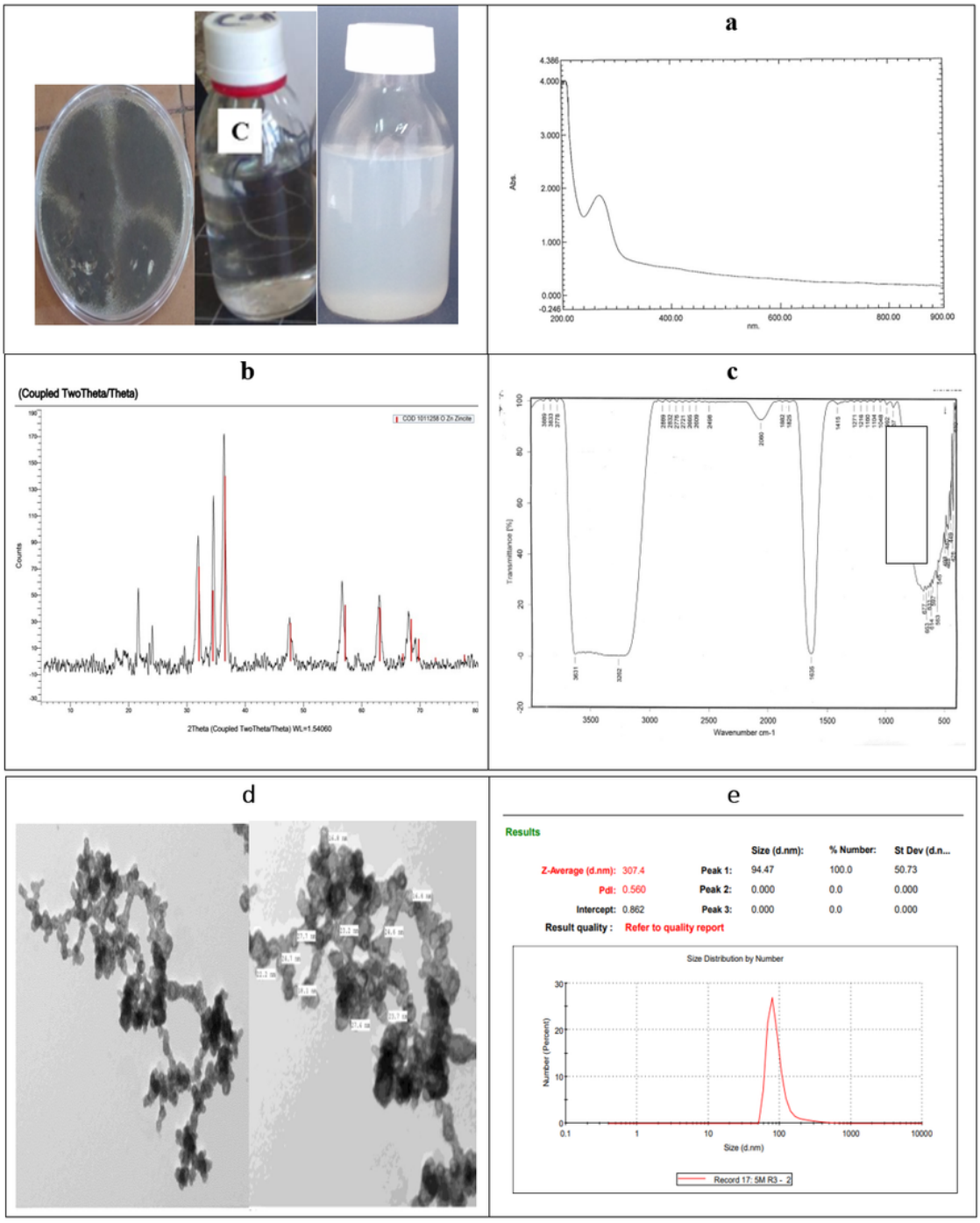

Figure 6

Characterization of the biosynthesized ZnO NPs utilizing *A. niger*, a) UV-Vis spectra, b) XRD, c) FTIR, d) TEM, and e) Zeta size and Zeta potential.

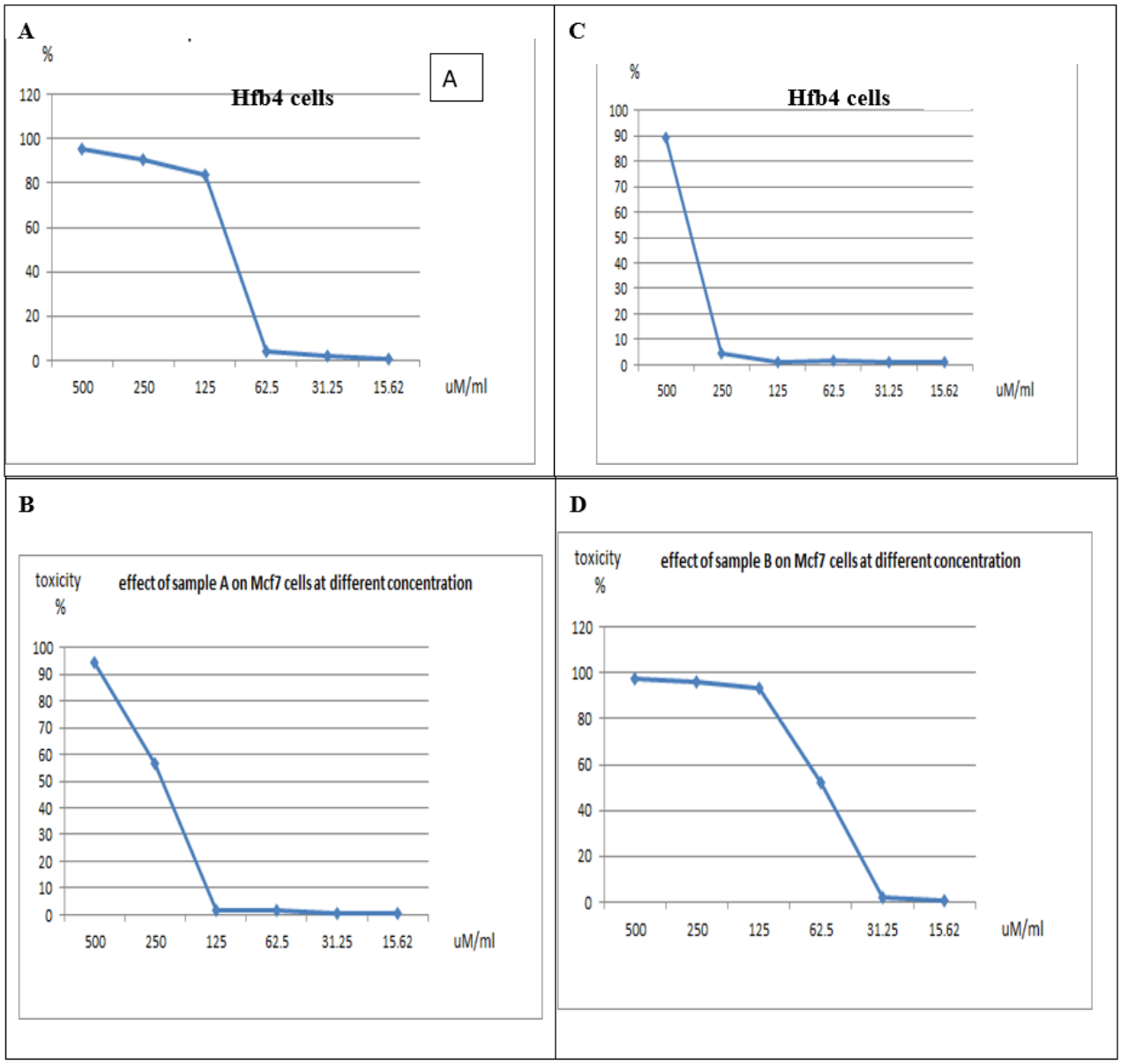

Figure 7

The impact of chemically synthesized ZnO NPs (A and C) and biosynthesized ZnO NPs by *A.-niger*(B and D) on Hfb4 and Mcf-7cell lines at different concentrations.

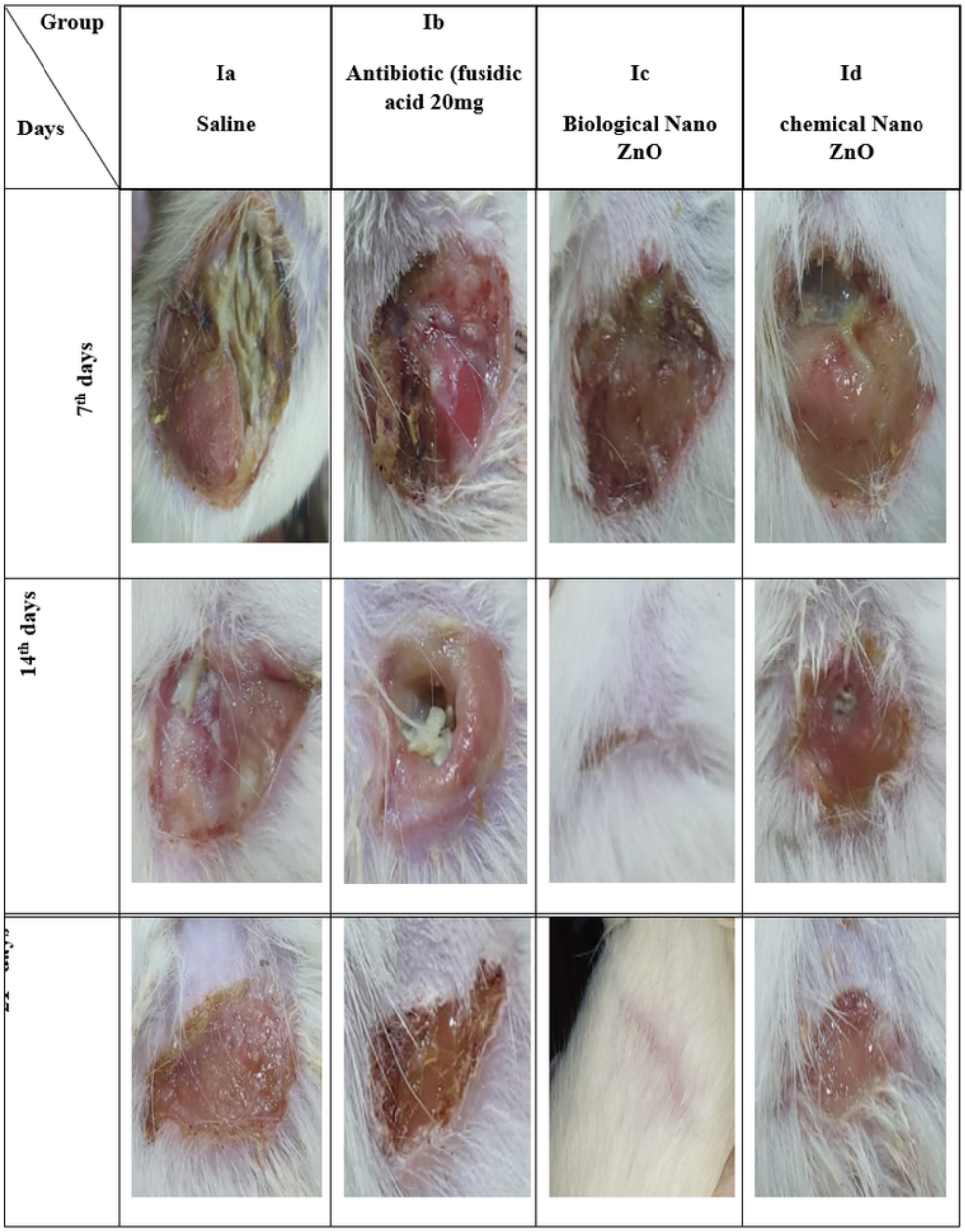

Figure 8

Efficacy of different antimicrobial agents against *P. aeruginosa.*

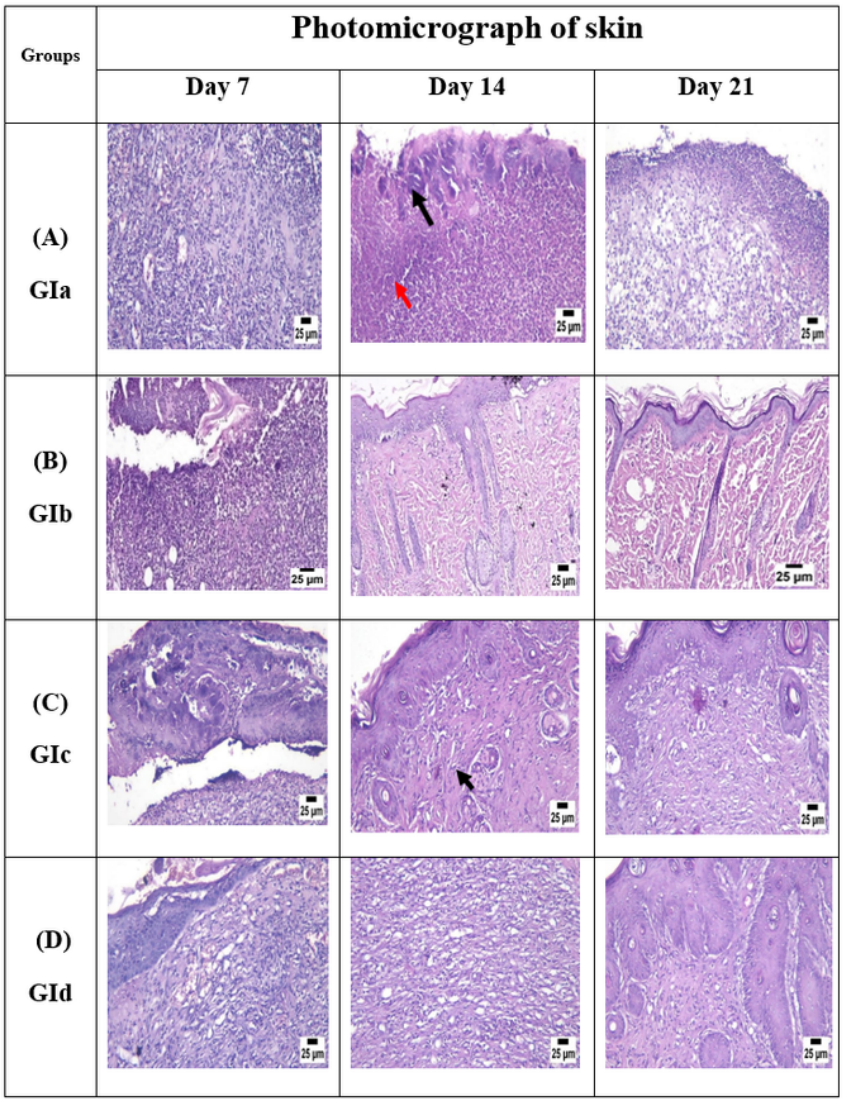

Figure 9

Rat skin photomicrographs showing a granulomatous response and a haemorrhage (red and blue arrows, respectively) (A) (wounded, infected, and treated with saline), (B) (wounded, infected, and treated with fusidic acid (20mg/100ml), (C) (wounded, infected, and treated with the biosynthesized ZnO NPs) and (D) (wounded, infected, and treated with the chemical ZnO NPs).